TALLINNA TEHNIKAÜLIKOOL
TALLINN UNIVERSITY OF TECHNOLOGY

Faculty of Mechanical Engineering

Department of Mechatronics

Chair of Mechanosystem Components

MHE70LT

Kirill Nuzhdin

Investigation of the Memristor Characteristics in Simulation of Friction Processes

Master's Thesis

Author applying for
master's sciences of technical
academic degrees

Tallinn
2015

AUTHORS DECLARATION

Hereby I declare that this Master's Thesis, my original investigation and achievement, submitted for the Master degree at Tallinn University of Technology has not been submitted for any degree or examination.

All works and major viewpoints of the other authors, data from other sources of literature and elsewhere used for writing this paper have been referenced.

Master's Thesis is completed under supervision of ....

“.......”....................201….

Author's

.... signature

Master's Thesis is in accordance with terms and requirements.

“.......”....................201….

Supervisor's

.... signature

Eligible for defence.

Chairman of defence committee ....

“.......”....................201…

.... signature

TALLINNA TEHNIKAÜLIKOOL
TALLINN UNIVERSITY OF TECHNOLOGY

Mehaanikateaduskond

Mehhatroonikainstituut

Mehhanosüsteemide komponentide õppetool

MHE70LT

Kirill Nuzhdin

Memristori karakteristikute uurimine hõõrdeprotsesside simuleerimisel

Autor taotleb tehnikateaduse
magistri akadeemilist kraadi

Tallinn

2015

AUTORIDEKLARATSIOON

Deklareerin, et käesolev lõputöö on minu iseseisva töö tulemus.

Esitatud materjalide põhjal ei ole varem akadeemilist kraadi taotletud.

Töös kasutatud kõik teiste autorite materjalid on varustatud vastavate viidetega.

Töö valmis Alina Sivitski juhendamisel

"15" mai 2015. a.

Töö autor

.... allkiri

Töö vastab magistritööle esitatavatele nõuetele.

".......".....................2015. a.

Juhendaja

.... allkiri

Lubatud kaitsmisele.

.... õppekava kaitsmiskomisjoni esimees

".......".....................2015. a.

.... allkiri

TUT Department of Mechatronics

Chair of Mechanosystem Components

MASTER'S THESIS SHEET OF TASK'S

Year 2015 spring semester

Student: Kirill Nuzhdin 150702MV
Curricula: MAHM - Mechatronics
Supervisors: Prof. Victor M. Musalimov, ITMO University
Teaching Assistant PhD Alina Sivitski, TUT

MASTER'S THESIS TOPIC:
(in Estonian) Memristori karakteristikute uurimine hõõrdeprotsesside simuleerimisel
(in English) Investigation of the Memristor Characteristics in Simulation of Friction Processes.

Thesis tasks to be completed and the timetable:

Nr	Description of tasks	Timetable
1.	Technical literature overview. Investigation of friction processes and electromagnetic phenomena in the friction.	15.02.2015
2.	Processing of tribological experiment results of different materials. The model production of friction process.	01.03.2015
3.	Memristor phenomena theory analysis. Investigation of operation theory and the memristor properties.	20.03.2015
4.	Memristor modeling in MATLAB for studying of friction characteristics.	15.04.2015
5.	Conclusions. Results.	10.05.2015

Solved engineering and economic problems: The aim of this Master's Thesis is investigation of the electrical phenomena occurring in friction processes. It's necessary to provide a method of using memristor for studying of electromagnetic phenomena in friction and produce more accurate models of solid friction. To understand the nature of origination of electromagnetic phenomena in the process of frictional interaction of bodies. Find a regularity which connecting the tribological characteristics tribosystem with electromagnetic phenomena occurring in friction.

Additional comments and requirements: …………………………………..............................

Language: English

Application is filed not later than 12.05.2015.

Deadline for submitting the theses 22.05.2015.

Student: Kirill Nuzhdin /Signature/ ……….. Date ……….........

Supervisor: PhD Alina Sivitski /Signature/ ……….. Date ……….........

Confidentiality requirements and other conditions of the company are formulated as a company official signed letter

Foreword

I received the theme of this work at the Department of Mechatronics at the ITMO University. This theme interested me, because it is a new and poorly understood. Currently, there aren't much works, which are linking electromagnetic phenomena and friction processes. For this reason, I believe that this topic is very relevant and the solution of the issues raised in this paper, will help to better understand the electrical phenomena occurring in the process of friction.

Acknowledgment

First of all, I would like to thank the head of the Department of Mechatronics of Tallinn University of Technology Professor Mart Tamre and the head of the Department of Mechatronics of ITMO University Professor Victor Musalimov for the provision of training opportunities in MSc Mechatronics Double Degree program. Also, I would like to thank my supervisors: PhD Alina Siwicki (TTU) and Professor Victor Musalimov (ITMO University) for his help in writing this work.

Kokkuvõte

Selle magistritöö teema arenes välja Sankt Peterburgi Rahvuslikus InformatsioonitehnoloogiaÜlikoolis (SPbNRU ITMO) koostöös Tallinna Tehnikaülikooliga (TTÜ). Teema oli esialgselt pakutud ITMO mehhatroonika õppetooli professor Viktor Mussalimovi poolt. Magistritöö põhieesmärgiks on hõõrdumisel tekkivate elektrinähtuste ning memristori karakteristikute uurimine hõõrdeprotsesside modeleerimisel.

Hõõrdumisel esinevate elektriliste nähtuste uurimine pakub suurt huvi eri materjalide hõõdre- ja kulumisprotsesside juhtimise teaduslikul põhjendamisel. Hõõrdumisel esinevad elektromagnetilised nähtused pole tänapäevani lõplikult läbi uuritud nende tekkeprotsessi komplitseerituse tõttu. Selleks, et saada täpsemat infot elektromagnetiliste nähtuste kohta, mis esinevad hõõrdeprotsessides (eriti metallide ja pooljuhtide tribopaaride korral) tuleb põhjalikumalt uurida tribokontakti ala, nimelt elektriliste karakteristikute parameetreid nagu takistus ja samuti hõõrde- ning termo-elektroliikumapanevat jõudude tekkepõhjuseid. Toetudes kaasaegsest eriala kirjandusest saadud teavele võib väita, et peaks olema võimalik leida seaduspärasus, mis seob hõõrdesüsteemide triboloogilised karakteristikud hõõrdeprotsessides toimuvate elektromagnetiliste nähtustega. Kõikide nende üleval nimetatud aspektide uurimine annab võimaluse avardada ettekujutust hõõrdumisega seotud seaduspärasuste elektrilistest komponentidest ja hõõrdeprotsessist üldiselt. Selles magistritöös esitatakse oletust, et memristor võib asendada tribopaari kontakti hõõrdeprotsesside modelleerimisel. Memristori rakendamine annab võimaluse uurida tribokontakti elektiahelate vaatevinklist.

Maistritöö esimene peatükk sisaldab sissejuhatuse ja ülesande püstituse. Teises peatükis esitatakse kirjanduse ülevaade hõõrdumisel tekkivatest elektrinähtustest. Põhirühk on termo- ja triboelektroliikumapanevate jõudude käsitlusel.

Teise peatüki lõpus kirjeldatakse ka elektriliste nähtuste mõju tribopaari kulumisele.

Kolmandas peatükis vaadeldakse memristori parameetreid ja karakteristikuid ning seletatakse lahti, milles seisneb memrtistori tööpõhimõte.

Neljas peatükk kirjeldab memristori mudeli ning selles esitatakse modelleerimise tulemused. Selles peatükis on samuti kirjeldatud erimaterjalide baasil loodud mudelid, mida kasutatakse memristorite valmistamisel.

Viiendas peatükis kirjeldatakse läbiviidud triboloogilised uuringud. Selles peatükis on esitatud meetod tribopaari kontakti takistuse muutuse seaduse muundamise funktsiooni saamiseks. Seda meetodit saab edaspidi kasutada hõõrdeprotsesside juures võrreldes näiteks hõõrdekontakri takistuse muutusi memristori elektriliste karakteristikutega. Peatüki lõpus on toodud graafikud pakutud funktsiooni rakendamisest.

Kuuendas peatükis on pakutud meetod memristori rakendamisest hõõrdeprotsesside modelleerimisel.

Kokkuvõtteks võib öelda, et teatud ajahetkedel tribopaari kontakti elektrilised karakteristikud (sealhulgas elektriline takistus ja voolupinge langus) suure täpsusega korduvad memristori elektrilisi karakteristikuid. Hõõrdeprotsessi käigus tekkivad elektromagnetilised nähtused avaldavad mõju tribopaari teatud hõõrdekarakteristikutele, mis annab võimaluse kasutada memristori hõõrdekontakti modeleerimiseks. Memristori ja tribokontakti karakteristikute võrdlemine annab võimaluse määrata hõõrdumisel esinevate elektrinähtuste parameetrid. See omakorda avab uued võimalused hõõrdekarakteristikute uurimiseks elektromagnetiliste ahelate teooria vaatevinklist.

Abstract

The work of this thesis was conducted during the training MSc Mechatronics Double Degree program between the Tallinn Technical University and St. Petersburg ITMO University. The head of the Department of Mechatronics of ITMO University Professor Victor Musalimov had offered the theme of this work. The main objectives of this master's thesis are the study of electrical phenomena occurring during the friction processes, also study of the characteristics of the memristor in the simulation of friction.

The substantial interest for science-based the process control of the friction and the wear are electrical phenomena in friction. Currently, the electromagnetic phenomena occurring in the process of the friction, not fully explored because of its complexity and of the unpredictable nature of the occurrence. In order to more fully explore the electromagnetic phenomena in the process of the frictional engagement of bodies (especially for friction pair consisting of a metal or semiconductor) are necessary to explore in more detail the tribocontact area, in particular its electrical parameters: contact resistance, and also the nature and occurrence of the thermal electromotive force and friction electrification. According to the modern literature, there is reason to believe that there is a dependence that connects the tribological characteristics of friction with the electromagnetic phenomena occurring in friction. The study of all these aspects makes it possible to expand the concept of the electric component of the laws of friction, as well as to more fully explore the process of the frictional engagement. Based on the approach which was proposed in this work, under the simulation of the process of friction, the memristor can replace the contact of the friction pair, also its using will be help in the investigation of the tribocontact in the context of electrical circuits.

The first chapter is represented an introduction and the statement of main objectives of the project.

In the second chapter, the review of literature devoted to the electrical phenomena occurring in friction was demonstrated. A special place was given to the phenomena of occurrence of the friction electrification and thermal electromotive force, also in the end of the chapter was described the influence of the electrical phenomena on the friction pair wear.

The third chapter was devoted to the memristor. It describes the main parameters and characteristics of the element, the device operation.

The fourth chapter describes the creation of the memristor model and the obtained simulation results. In addition, there was described the model based on various materials used in the manufacture of the memristor.

The fifth chapter is devoted to the results of the conducted tribological experiments. Also in this chapter is proposed a method of obtaining the transfer function of the law changes of the tribopair contact resistance for the later comparison with the electrical characteristics of a memristor. There were provided graphical results of using of this function.

In the sixth chapter was described the proposed method for using of the memristor under simulation of the friction processes.

In conclusion, it can be deduced that at certain times the electrical characteristics of the tribopair contact (in particular electric resistance and the drop in voltage) is repeating with high precision the electrical characteristics of the memristor. The electromagnetic phenomena occurring in the process of friction have an impact on the characteristics of the friction pair, it does not allow full use of the memristor to simulate the contact. However, comparing the electrical characteristics of the data (of the tribocontact and the memristor) may be determined the parameters of electrical phenomena in friction. This, in turn, opens up new horizons for the study of tribological characteristics in the context of the electromagnetic theory of electric circuit.

Table of contents

1. Introduction

1.1. Description of the problem domain

Friction as the aggregate of physical phenomena in the area contact of the tribological system is dissipative process, which is accompanied: heat release, electrification of rubbing bodies, tribochemical reactions, structural phase transformations in surface layers of friction parts, etc.

The electrical phenomena in the friction process have the significant interest for scientific rationale of the control of friction process. It is also necessary to study in greater detail the effect of external sources of electromotive forces and magnetic fields on the friction and wear processes. The published information about this is ambiguous and in some cases is contradictory.

Currently, electromagnetic phenomena occurring in the process of friction not fully explored due to its complexity and features of origination of these phenomena.

To solve this problem, there was suggested a theory, whereunder the memristor (passive nonlinear circuit element whose resistance does not depends up the voltage applied to it at a given time, but depends up the voltages or currents in all previous times) can be used in the simulation of friction processes. According of this theory, in the process of friction it may occur a moment when the electrical characteristics of the contact area of the tribopair with a high degree of accuracy will be repeating the electrical characteristics of the memristor. The tribopair in this time is regarded as kind of the memristor.

1.2. Problem statement

In order to better understand the nature of origination of electromagnetic phenomena in the process of frictional interaction of bodies (especially for friction pair consisting of a metal or a semiconductor) is necessary to explore in details the area tribocontact, in particular the parameters of the electric type: the contact resistance, friction electricity (triboelectricity) and thermo-emf.

Another important aspect is the analysis of the effect of the tribological characteristics, such as the force of friction, the wear, the friction coefficient and others on electromagnetic processes occurring in friction.

Also, there are grounds for believing that there is a regularity which connecting the tribological characteristics tribosystem with electromagnetic phenomena occurring in friction. The investigation of all these aspects makes it possible to extend the understanding the influence of the electric component on the laws of friction, and in further detail explore the process of frictional interaction.

1.3. The work objectives

During the pursuance of the research, I had the following main objectives:

1. The investigation of electromagnetic phenomena occurring in friction processes;
2. The research of properties and characteristics of a memristor;
3. The search of a relationship between the change of the electrical characteristics of the contact tribopairs and characteristics of the memristor (particularly resistance).

2. Electromagnetic phenomena occurring in friction processes

This chapter provides a review of the literature devoted to the study of electrical processes in friction. Here are characterized the basic electrical phenomena occurring in the process of friction and given their impact on the tribological characteristics of friction pairs.

2.1. Electrification Processes

The appearance of origination of static electricity during the friction process (triboelectrification) has been known for thousands of years. Contacting of two materials is sufficient to instigate the electrification. Friction is common a type of interaction which doing enlargement of the area of contact and generates heat - friction is the general term to explain the movement of two objects in contact; the pressure exerted, its shear velocity and the heat generated are the prime determinants of the charge generated by friction. In certain circumstances the friction will lead to the tearing away of solid particles as well.

When the two solids in contact are metals (metal-metal contact), electrons migrate from one to the other. Every metal is characterized by a different initial potential (Fermi potential), and nature always moves towards equilibrium - that is, natural phenomena work to eliminate the differences in potential. This migration of electrons results in the generation of a contact potential. Because the charges in a metal are very mobile (metals are excellent conductors), the charges will even recombine at the last point of contact before the two metals are separated. It is therefore impossible to induce electrification by bringing together two metals and then separating them; the charges will always flow to eliminate the potential difference.

When a metal and an insulator come into nearly friction-free contact in a vacuum, the energy level of electrons in the metal approaches that of the insulator. Surface or bulk impurities cause this to occur and also prevent arcing (the discharge of electricity between the two charged bodies the electrodes) upon separation. The charge transferred to the insulator is proportional to the electron affinity of the metal, and every insulator also has an electron affinity, or attraction for electrons, associated with it. Thus, transfer of positive or negative ions from the insulator to the metal is also possible. The charge on the surface following contact and separation is described by equation [1]:

$$\sigma_s = e \cdot N_E \cdot (\varphi_m - \varphi_i) \quad (1)$$

where σ_s - the surface charge density following contact and separation; e - the charge of an electron; N_E - the energy state density at the insulator's surface; φ_m - the electron affinity of the insulator; φ_i - the electron affinity of the metal.

When two insulators come into contact, charge transfer occurs because of the different states of their surface energy [1]:

$$\sigma_s = e \cdot \frac{N_{E1} \cdot N_{E2}}{N_{E1} - N_{E2}} \cdot (\varphi_1 - \varphi_2) \quad (2)$$

where N_{E1} and N_{E2} are the energy state densities at the surface of the two insulators; φ_1 and φ_2 are the electron affinities of the two insulators.

Charges transferred to the surface of an insulator can migrate deeper within the material. Humidity and surface contamination can greatly modify the behaviour of charges. Surface humidity in particular increases surface energy state densities by increasing surface conduction, which favours charge recombination, and facilitates ionic mobility. Most people will recognize this from their daily life experiences by the fact that they tend to be subjected to static electricity during dry conditions. The water content of some polymers (plastics) will change as they are being charged. The increase or decrease in water content may even reverse the direction of the charge flow (its polarity).

When a solid and a liquid meet (to form a solid-liquid interface), charge transfer occurs due to the migration of ions that are present in the liquid. These ions arise from the dissociation of impurities which may be present or by electrochemical oxidation-reduction reactions. Since, in practice, perfectly pure liquids do not exist, there will always be at least some positive and negative ions in the liquid available to bind to the liquid-solid interface. There are many types of mechanisms by which this binding may occur (e.g., electrostatic adherence to metal surfaces, chemical absorption, electrolytic injection, dissociation of polar groups and, if the vessel wall is insulating, liquid-solid reactions) [1].

2.2. Frictional electricity

Friction is the force resisting the relative motion of solid surfaces, fluid layers, and material elements sliding against each other [2].

A considerable amount of research of electromagnetic phenomena in the process of friction and wear are represented in modern literature. Triboelectric and thermoelectric phenomena collectively influence on the wear of all the tribosystem elements. That phenomena together with the mechanical wear will largely reduce the resource.

Electromagnetic phenomena accompanying the friction process implement in all tribosystems and under all types of friction (dry, fluid, lubricated). Always in the sliding process the both specimens is electrified [3].

During the friction of dielectrics, semiconductors or conductors (having different or identical composition), during the mutual friction of liquid dielectrics, etc. is always electrifying the both bodies which involved in the process of friction. Their charges have the same value and different signs.

Electrification under friction has a number of consistent patterns. Firstly, during friction of two chemically identical bodies, the specimen with a higher density gets the positive charge. Secondly, electrification of bodies is directly proportional to the surface area of contact. Thirdly, in the process of friction between two solids are occurring a local contact and subsequent separation of these areas. At the moment of contact, the electrons and ions are moving from one body to another. The contact electrification of the two metals or metal and semiconductor was generated in consequence of the transition of electrons across the interface from the body with less energy exit of electrons to the body with bigger energy exit of electrons (contact voltage). In the case of contacting the metal with a dielectric the electrification occurs in consequence of the transition of electrons from a metal to an insulator and positive ions of the dielectric to the metal surface. It the process of contact of two dielectrics, electrification is a consequence of the diffusion of charge carriers from one material to another.

In the study of tribological phenomena occurring in dry friction process of metals under the reciprocating movement were observed the formation and accumulation of significant electrical potentials, as shown in Figure 1.

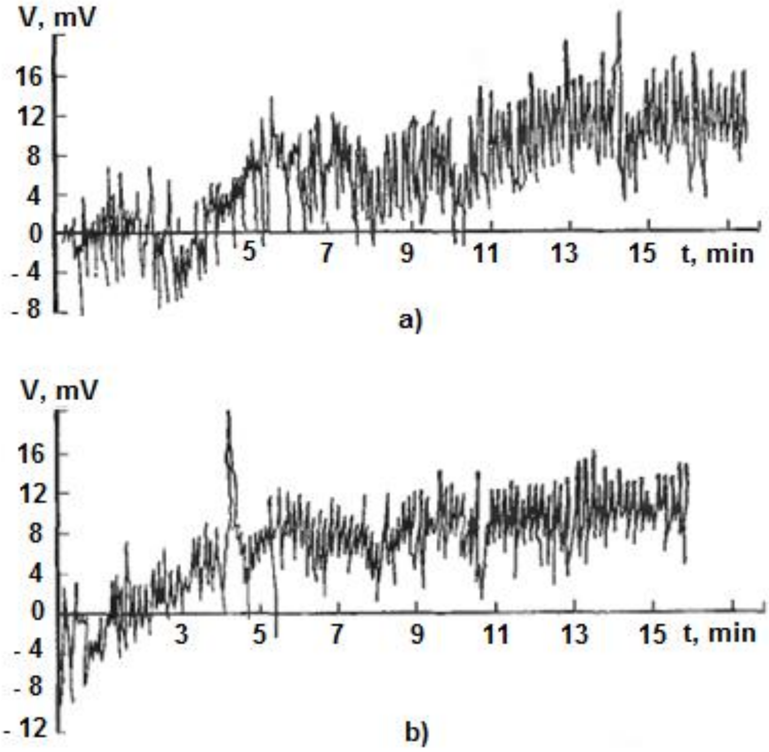

Figure 1 - Voltage was created during solid friction processes: a) F_{normal} = 66 N, b) F_{normal} = 96 N; materials: Steel 45 – Teflon; speed: v = 1,42 m/s [5]

Introduction of the dielectric (oil or lubricant) between the two mutually moving conductors leads to the formation of a kind of capacitor in which electric charges are accumulated (shown in Figure 2).

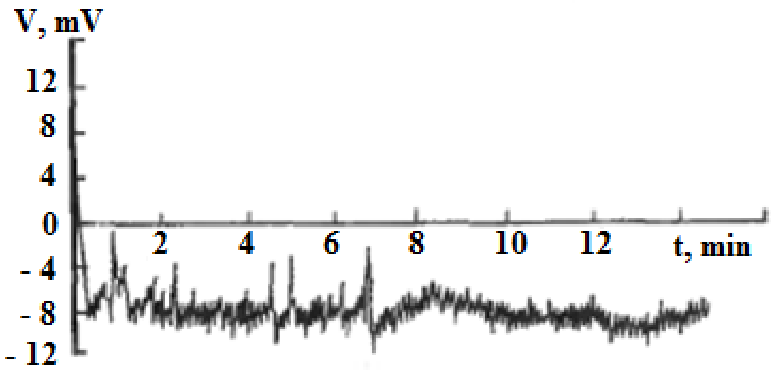

Figure 2 - Voltage was created during the lubricated friction process (F_{normal} = 96 N; materials: Steel 45 – Teflon; speed: v = 1,42 m/s; lubricant: "bright stock") [5]

Also other electrokinetic phenomena can have the specific influence. During friction, the lubricant film may be broken because of short-wavelength pattern, consequently it may origination of electrical phenomena, especially under high loads. They are similar to phenomena under dry friction: the emission of electrons, thermoelectric effects, contact-potential difference, etc.

As a result of rapprochement microroughnesses of the electrified surfaces, on the some distance may occur a local dielectric breakdown and a transport of electric charges from one surface to another, this is similar to atmospheric discharges. The moving electrical charges is becoming a source of magnetic field. The magnetic field, in turn, is a form of electromagnetic field which acting on the body with an electric charge or the body is having a magnetic moment, regardless of whether they are moving or are dormant [4].

In the works of M.T. Balabekov experimentally was established a regularity in the sequence of energy, according to which, the work of friction forces in the first act of interaction is spent on education of the electromagnetic field and only then generates heat. By virtue of the fact that the acts of the friction engagement follow each other and at the same time in different parts of the contacting surfaces, then in the real tribosystem the electrical and the thermal processes develop simultaneously contributing to the change in the energy state of the system. The author of this work had carried out to study the electrical phenomena in metal-polymer tribosystem during the friction of sample made of polymeric composite material on the metal counterface according to the scheme pin-on-disk (Figure 3) [5].

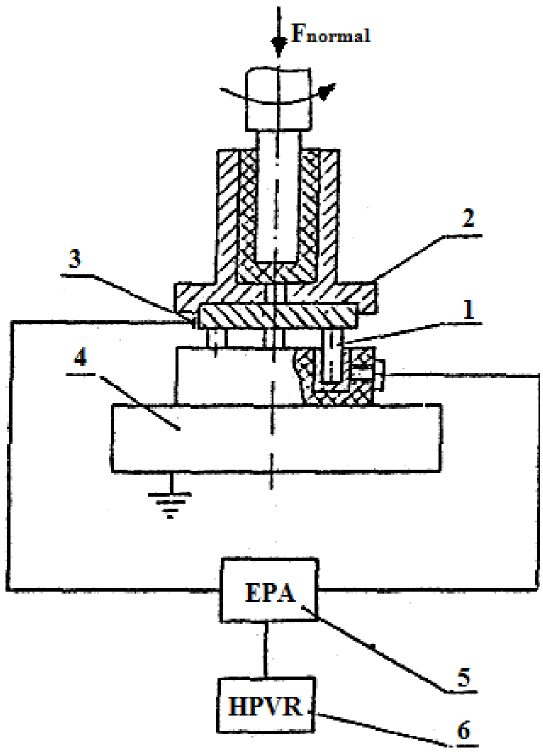

Figure 3 - The measurement scheme of tribo-electromotive difference of potential: 1 - samples made of polymeric composite material; 2 - counterbody; 3 - slider contact; 4 - the base stand; 5 - electric pulse amplifier; 6 - high-precision variable resistor [5]

In the process of friction, there was measured the potential difference and the current between the polymer specimens and the metallic counterbody, which were used to calculate the amount of electricity (charge) and the electric field in the condenser, where a polymer specimen served as a gasket. The tests were performed for the two composite materials based on polytetrafluoroethylene (WHC-3 and kriolon-3) and for two types of counterbodies made of alloy B95, that differ the surface pre-treatment. One line of the counterbodies was exposed to only the action of the chemical etching using the solution of NaOH after a mechanical conversion. Additionally, the second line of the counterbodies was exposed to the action of an implantation doping. The experimental results showed that the highest amplitude of the electric field are observed for the counterbodie which was modified ion implantation and material kriolon-3. This indicates that the friction pair has a biggest efficiency characteristic of the electrophoretic process and, therefore, there is the least number of the wear products in the friction zone [6].

The graphs (Figure 4) which was obtained by the automatically recorder for high-precision variable resistor is characterizing the vibrational behavior of the change difference of electric potential between the polymer samples and the counterbody. Figure 4 (a) shows a curve of the change difference of electric potential under steady state the friction process which is corresponded to the stationary thermodynamic state of the tribosystem. The character of the curve in Figure 4 (b) is significantly different from the curve in Figure 4 (a). This fact indicates the presence of the transition process in the system with low-frequency changes of the difference of electric potential and with overlapping to them vibrations of higher frequency. The transient phenomena can be caused by external disturbances (increased load, sliding velocity, etc.) or by internal processes associated with the formation and destruction of the surface structure of the polymer sample etc.

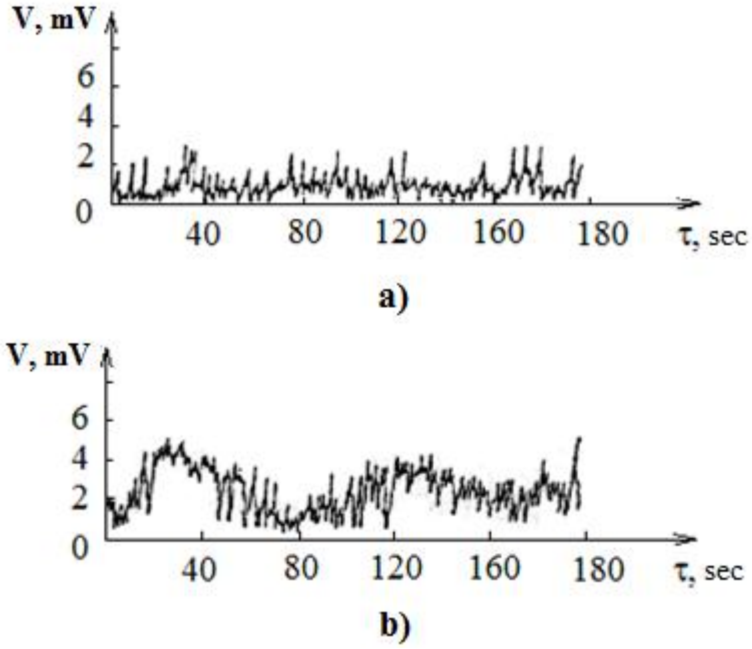

Figure 4 - Curves of the triboelectricity under steady (a) and transient (b) friction conditions [6]

The oscillatory behavior of the change of the electromotive difference of potential in metal-polymer tribosystem is remained regardless of the type of the investigated polymeric composite material, processing method (modification) of the surface of the metal counterface. Obviously, these oscillations of the difference of electric potential are expressing the internal dynamical behavior of the physicochemical processes in the mechanism of friction and wear of metal-polymer tribosystems. The presence of the stable oscillations electrophysical parameters and transients in the tribosystem indicates that in the system is implemented the negative feedback, which ensures the stability of self-oscillatory processes. It is fair to assume that other physicochemical processes in friction (thermal, chemical, destructively-structure-forming, etc.) have the oscillatory in nature, but to reveal its technically much more difficult than the revelation of the fluctuations of electrophysical parameters.

In the research paper [6] there was investigated the dependence of the tribo-electromotive difference of potential on the contact pressure $V = f(p)$ for different values of constant temperature and the dependence of the tribo-electromotive difference of potential on the temperature $V = f(T)$ for different values of constant pressure (Figure 5).

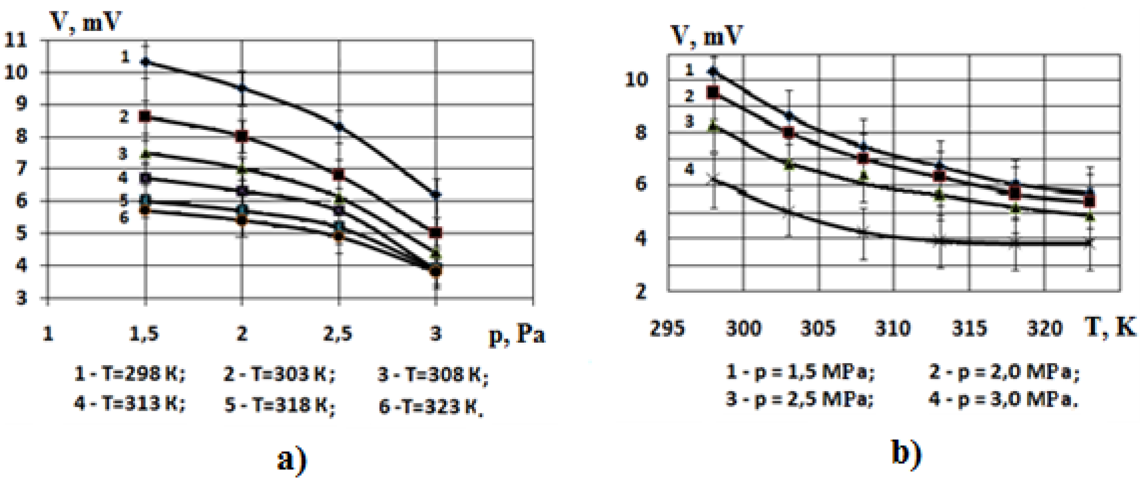

Figure 5 - The dependence of the tribo-electromotive difference of potential: a) on the contact pressure $V = f(p)$; b) on the temperature $V = f(T)$ [6]

The obtained results show that increase of the contact pressure leads to reduction of tribo-electromotive difference of potential (Figure 5 (a)), and also it reduces the temperature gradient of tribo-electromotive difference of potential (Figure 5 (b)).

The results of polynomial approximation showed that in the temperature range from 298 K to 323 K the dependence of the tribo-electromotive difference of potential on the contact pressure can be described by equations [6]:

$$V = a \cdot p^3 + b \cdot p^2 - c \cdot p + d \quad (3)$$

where a, b, c, d are coefficients specific to a particular contact pressure and temperature.

Also found that the tribo-electromotive difference decreases with increasing temperature and the higher the temperature, the smaller the difference between different values of the tribo-electromotive difference under contact pressure.

The character of the obtained experimental dependences $V = f(T)$ for polymeric composite material which made of crystalline amorphous polymer PTFE (polytetrafluoroethylene) can be explained with the assistance of the provisions of the band theory, according to which the electronic work function of the polymer decreases with increasing temperature, thereby reducing the tribo-electromotive difference.

During the operating conditions of tribosystems the contact pressure and the temperature in the zone of friction often change simultaneously. Therefore the dependence of the tribo-electromotive difference on the contact pressure and the temperature was tested by implementing of factorial experiment. After that, there was obtained the regression equations in the code values [6]:

$$V = 4.9 - 1.0 \cdot x_1 - 0.25 \cdot x_2 \quad (4)$$

where x_1 is the contact pressure; x_2 is the temperature.

From the equation it follows that the contact pressure has a much greater impact on the value of the tribo-electromotive difference than the temperature. Increasing pressure and temperature leads to a decrease the tribo-electromotive difference.

2.3. Thermal electromotive force

In the electrification process the rise of temperature of friction pair has a significant importance. If the surface of one of the specimens has a temperature greater than the other, charge carriers are transferred from one specimen to another, consequently that create thermoelectric current [5].

It is notorious that due to the intense heating of rubbing surfaces of metal specimens, their area of direct contact can be regarded as a hot junction of the thermocouple element.

Record of electromotive force (shown in Figure 6) which is generated during the friction of specimens can provide information about the average temperature on the friction surfaces and characterize the dynamic physical processes of the friction mechanism.

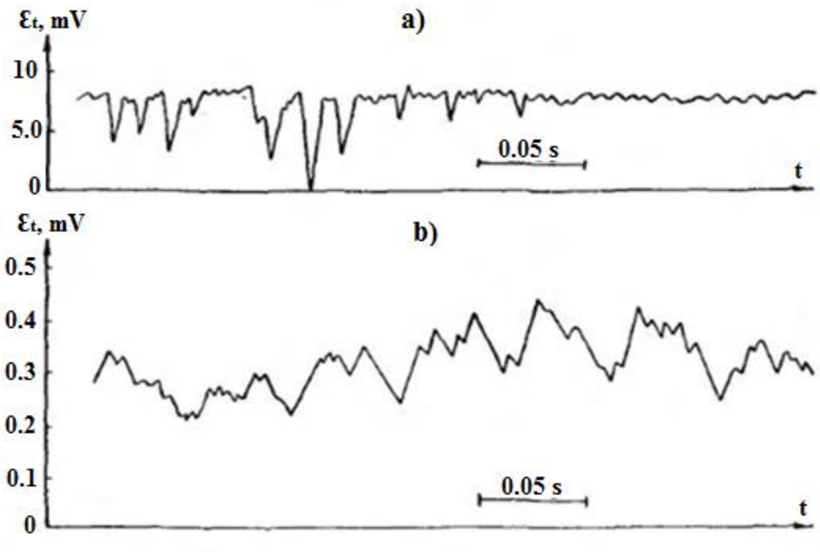

Figure 6 - Oscillograms of electromotive force for friction pairs: a) Constantan - Copper; b) High carbon steel - Low carbon steel [7]

The macroscopic study of electrical phenomena in friction processes becomes more systematic, if we use the integration of schemes of the nonlinear electric circuits with variable parameters that meet any of the elementary acts of frictional interaction.

Supposing that four roughness peaks have metallic contact under the process of relative sliding of solids. In this case the internal thermoelectric circuit is formed, as shown in Figure 7. During the friction process it may be that the temperature of both contact areas are not the same ($t_1 \neq t_2$), and in a closed circuit made up of the conductors I and II (r_1 and r_2 - contraction resistance areas) will act the thermoelectric power e_t. The electromotive forces generated by the temperature difference in both branches of the circuit may act not only opposite (the same conduction mechanism of metals I and II), but also combined (the circuit is composed of the electrical conductors and the hole conductors).

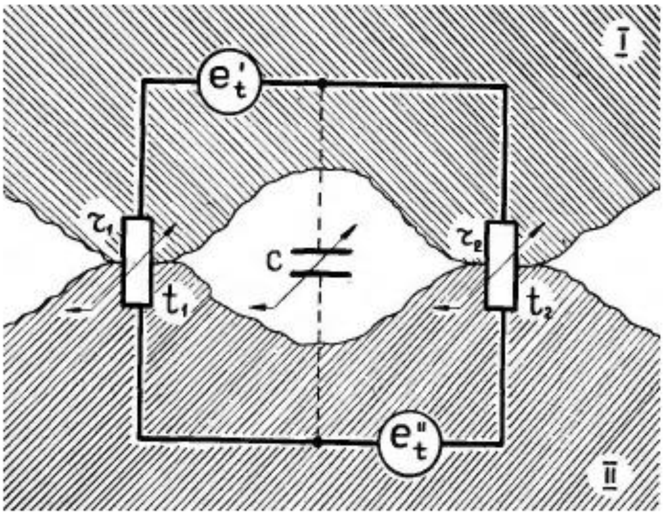

Figure 7 - The unit of contact cell and the scheme of its thermoelectric circuit [7]

Also in Figure 7 we can see the nonlinear parametric capacitance *C*. Its value depends on the distance between the friction surfaces and the dielectric constant of the medium filling the interfacial slit space. Differential capacitance and "single-turn" circuit inductance characterize the state of the electromagnetic field of the frictional capacitor.

In the real contact takes place a group of loop thermoelectric currents i_1, i_2, ... , i_n as shown in Figure 8. On the surfaces of polycrystalline metals may flow a local microcurrents due to the difference of work function of crystal faces.

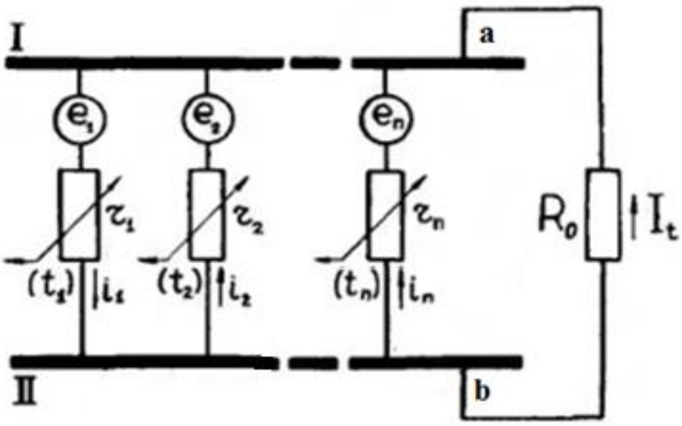

Figure 8 - Internal and external thermoelectric circuit of the friction pair [7]

The total resistance of the discrete contact [7]:

$$R_m = \frac{1}{\sum \frac{1}{r_i}} \tag{5}$$

where r_i *(i = 1, 2, ... , n)* — the resistance to one of the contact area. The hot junction of the thermocouple element comprises a few thermocouples connected in parallel. If the external circuit of the friction pair closed onto the contact resistance R_0 and e_i is the electromotive force of the outer circuit, then the instantaneous average value of the resulting thermal electromotive force[7]:

$$\mathcal{E}_t = \sum_{i=1}^{n} e_i g_i \Big/ \sum_{i=1}^{n} g_i \tag{6}$$

where g_i *(i = 1, 2, ... , n)* — the conductivity of the *i-th* the contact area.

Total thermoelectric current [7]:

$$I_t = \frac{\mathcal{E}_t}{R_m + R_0} \tag{7}$$

2.4. The modern views on the mechanism of electrification by friction

It is known that the true friction electrification occurs only under the asymmetric friction of chemically identical materials [8]. It may be associated with different propagation velocity of the charge across the surfaces of the friction bodies due to their different temperature gradients [9]. In most cases, the bodies electrification during the friction process is caused by the so-called the contact electricity. The process of friction leads only to an increase in the number of contact areas. However, it must be borne in mind that the effects inherent to the friction process may have a significant impact on the behavior of the transition of electrons or ions through the surface of the interface, and even change the mechanism of contact electrification.

Only in relation to the contact of the two metals, two semiconductors, metals and semiconductors we can talk about the clear understanding of the mechanism of redistribution of charges. The contact electrification in this case is characterized the prevailing transfer of electrons through the interface from the substance with a lower work function to a substance with a high work function. As for the dielectrics, the literature review indicates some uncertainty and even contradictory points of view on the mechanism of contact electrification. It is believed, for example, that when a metal and a dielectric are making contact, the electrification is characterized the transition of electrons from the metal to insulator transition and the transition of positively or negative ions on the surface of the metal. During the contact of two dielectrics, the electrification occurs due to diffusion of charge carriers from one material to another. The physical-chemical "dirt" and wear debris in this case is regarded as a supplementary factor that may distort the phenomenon of electrification, but do not change its nature.

The possibility of a different approach to the question of static charge is indicated in [10]. It is also noted that the transfer of ions plays an important role in the electrification of the solids, but the preference is given to those of the mobile ions, which were formed as a result of electrolytic dissociation in the surface film of moisture. It is believed that the gap of double diffusion layer of the electrolytic ions in a thin film of water between the two dielectrics (metal and dielectric) is the cause of electrification of the separable from each other surfaces. In other words, the dielectric can't obtain a significant charge during the acts of frictional interaction; the dielectric will be able to become electric only when it has "the electrolytic mud".

The original solution of the mechanism of friction electrification dielectrics was invented Kornfeld [11]. The decision was based on the hypothesis, according to which, the solid dielectrics (ionic crystals, amorphous polymer and bodies) have the own electric charge. In addition to studies of the Kornfeld, the presence of such a charge is confirmed by the results of other experimental works. According Kornfeld, the compensation of the intrinsic charge of the dielectric is occurring due to selective adsorption of ions of opposite sign. Therefore, the physical-chemical "dirt" on the surface of the dielectric is charged. During the friction of two samples the layers of dirt are mixed and redistributed between the rubbing surfaces. Compensation of the own charges is violated, which is the reason of friction electrification [7].

2.5. The influence of electric current on the wear during the friction processes

For the first time, the negative effect of electric current on aged deterioration was found during the friction process. Brothers Gordienko in 1952 investigated the electrical phenomena in friction of metals and their impact on the wear of metal bodies [12]. They showed that the electric current in friction process occurs due to the occurrence of a thermoelectric power in a closed circuit which is formed by a friction pair. According to the work [12], the lowest wear of patterns are observed by using the electrical insulation of samples, the largest wear - during introduction of the electric current (of the same polarity as that of the current in the thermoelectric system) in a friction zone. Brothers Gordienko advanced a hypothesis which was explaining the negative effect of electric current on the wear during th friction process with the electroerosion destruction.

In the work [13] was shown, that the effect of electric current on the wear by friction of samples differs depending on the magnitude and direction of the electric current in the system. In particular, the authors have shown that the wear is significantly reduced when there is applying the current with polarity which is the reverse polarity of the electric current in the pair of friction and greater in magnitude than the electric current in its own system.

The authors of the work [13] have shown, that the electric current during the friction process affects on the processes of oxidation which is occurring on the rubbing surfaces. In such a case, authors indicate that the influence of electric current on the metal wear during the friction was induced for the most part largely of the electromigration phenomena, but not the electroerosion destruction, as previously indicated Gordienko. The authors substantiate the idea, that during the friction process of metals the thermoelectromotive force isn't exceeding tens of millivolts, and the electric current - a fraction of milliampere,therefore, the charge which is originated at the contact areas, it is not powerful enough to cause a considerable wear.

Afterwards, the studies in this direction were continued and developed by M.T. Galey [14]. In his work, he points out that an indispensable prerequisite for the creating of electric current is the chemical heterogeneity of the materials which is contacted. He has shown that thermoelectromotive force are changing by change of the parameters of cutting mode or of the friction process. Galey also indicates the existence of a linear correlation between the thermoelectromotive force and temperature, based on the law Seebeck [14]:

$$E = \int_{T_1}^{T_2} S_A dT - \int_{T_1}^{T_2} S_B dT = \int_{T_1}^{T_2} S_{AB} dT \quad (8)$$

where *E* - the thermoelectromotive force, mV; *T* - the temperature gradient, °K; S_A and S_B - coefficients of the thermoelectromotive force of the materials thermocouple, which equal potential difference is originating on the ends of the conductors, when they are placed in a temperature field with a temperature difference on the ends of the conductor, which equal to one Kelvin degree, mV/°K.

Galey provides the data which assert that frictional wear depends upon the direction of electric current in the circuit. He showed that the applying of electric current (in a direction opposite of the current in the existing system) in the closed electrical circuit is causing the decrease of the wear of the specimens of steel P18 by almost half. The feature of the work [14] is that the author tries to link the thermoelectromotive force with the thermal phenomena occurring in friction, and shows that there is a correlation between a direction of electric current in the system and the cooling in the sites of friction, which is connected to the Thomson effect.

Thus, in the early studies of thermoelectric phenomena in friction it has been revealed that the electric current has a complex impact on the wear of friction pairs. According to the authors of [12, 13, 14] the electric current leads to an intensification of electrosparking, electrodiffusion and oxidative wear.

The phenomenon of hydrogen wear in most cases also has an electrochemical nature and it is determined the electrode potential of the metal. In the work [15] were analyzed the electrochemical positions of the possible conversions on the frictional contact, which lead to the formation of free hydrogen. The friction, on the one hand, accelerates the desorption of hydrogen from the surface, and on the other - enhances the ability of the metal to absorb hydrogen. Usually, during the friction, the potential is shifted in the cathode region, this promotes more intensive excretion of hydrogen.

The exoelectronic emission (Kramer effect) - the process of electron emission from the surface of solids as a result of excitation of surface from deformations during various types of processing, as well as a result of irradiation of the sources of different physical nature (y-rays, ultrasonic waves, etc.) [16].

The research data of the intensive exoemission dry friction show that using the emission curves, which were obtained in the dynamics friction, you can get information about processes in the contact area, to assess the condition of the friction surfaces and the level surface free energy and to study regularities of the reverse friction. In [16] was found that at the initial moment of the friction process, the exoemission intensity and the toughness are increased, but the electron work is reduced. During the reverse friction, this regularity is broken. The decrease of the electron work in the reverse process corresponds to an increase exoemission (the places clusters of structural defects are its center).

Consider in more detail the thermoelectric phenomena in conditions of contact interaction in friction, which can be called triboelectricity.

Study of occurrence of jumps frictional force [17] showed that the cause of the jumps are electrostatic phenomena in the layer of grease and the contact surfaces of the metal elements of the friction pair. The dielectric properties of the lubricating film determine the values of the breakdown voltage (15-20 kV) and the current flowing through the contact. The authors suppose that a significant contribution makes a contribution to the general friction force, it is necessary to have the higher current density for the provide of the smooth, without jumps, sliding motion.

As a result of an analysis of the electric current during the friction [18, 19], it was found that the electric current occurs even if the friction samples are produced from the identical materials. This enabled the authors to conclude that during the friction of solids the electric current flows due to the thermoelectric power and thermionic emission. Observed the average values of the current during the friction process of plates made of various metals, with and without lubrication, have shown that the magnitude and direction of the current are diverse for different metals.

As shown in work [19], the thermionic currents are a crucial factor in the amount of wear conjugate pairs. To test the effect of the electric current on the wear of friction of samples were carried out long-term test [19] samples at normal operating conditions and applying of the short-circuit shunt. Under the identical operating conditions, the wear resistance of friction pairs with a shorting shunt (the partial compensation thermopower) is twice as much as the wear resistance of samples without shunt (Figure 9).

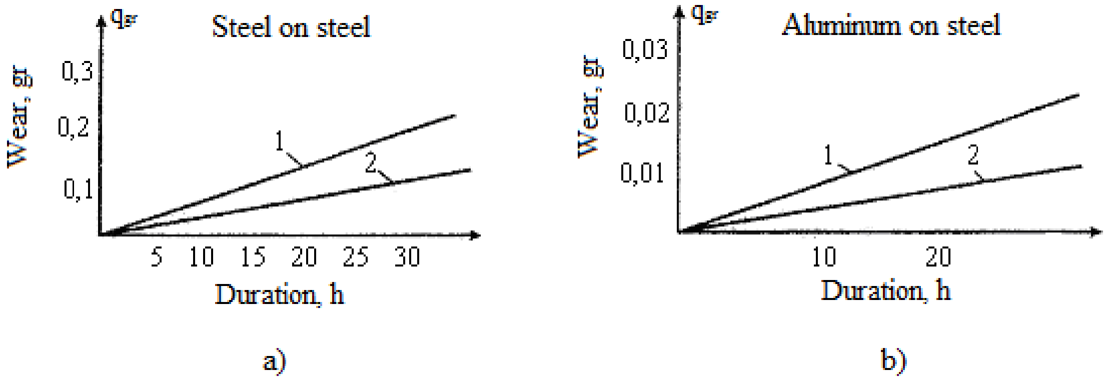

Figure 9 - The wear of the rubbing surfaces of steel and aluminum specimens: a) operating without a shunt; b) when a shunt is applied [18, 19]

The similar results were obtained when the direct current by an external source was administered at the friction zone. It was found that the potential fluctuation is minimum by a current of 80-120 μA. For each pair of friction there is an optimal value of the current. In a production environment the studying the influence of the current depreciation of the spinneret shown that the resistance of the spinneret with the connected capacitor is 3 times higher than their resistance when operating under normal conditions.

Effect of electric current on the wear in the friction is investigated in work [20], where the wear of the specimens of straight bronze during the half-floating condition with the end wall of tempered steel disc. Simultaneous the two samples, which were separated from each other and the unit casing, were subjected the test, but the wear was determined on one sample. The experiments were carried out under speed V = 12,5 m/s and specific pressure p = 1.6 kgs/cm^2 in the presence of lubricant (the technical petroleum jelly) on the friction surfaces. It was determined the influence of the current from an external source (I = 6 A, E = 1 V) and its direction of the sample wear, as well as thermoelectric current, arising during insulation test sample on the site of friction. According the author, in this case the thermoelectric current was smaller than for the two samples, and occurs in consequence of the velocities difference of the friction on different sections of the friction surfaces.

In Figure 10 is shown, that the greatest wear occurs when the current is flowing from the abradable sample to the disk (Figure 10, a). Under the reverse polarity (Figure 10, b) the wear of the sample is decreased 4 times. The lowest wear was observed when the abradable specimen isn't part of the electrical circuit (Figure 10, c) and the wear about 1.5 times lower than in the closed circuit (Figure 10, d).

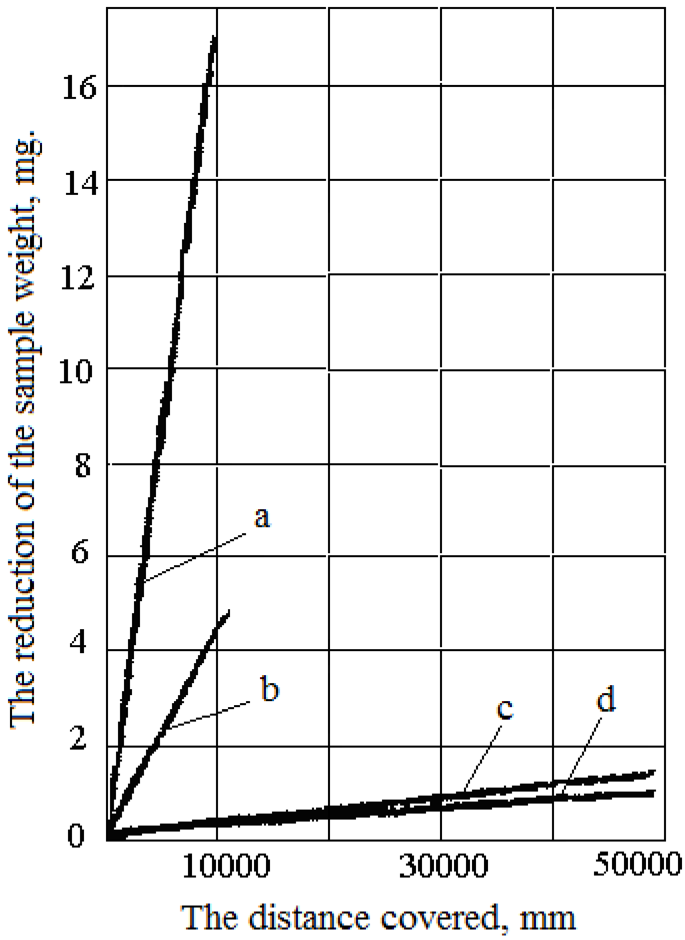

Figure 10 - The influence of electric current on the wear during the friction of the patterns made from the tin bronze and the hardened steel: a - the sample was attached to the positive terminal of the battery; b - the sample was attached to the negative terminal of the battery; c - the circuit thermoelectric closed; d - the sample isolated [20]

Summing up the preliminary results of the review of the impact of the domestic energy impacts on the friction and wear, was observed that these phenomena are studied at the macro-, micro- and submicro-layers. Above all, the point at issue is that the influence of triboelectric processes on the wear, whose of the regularity on each of these levels untill isn't investigated enough.

At the micro level also marked synergistic effects, for example, such as the frictional electricity (thermophysical phenomena). When used in respect of the submicro-layer the optimal density of dislocations, which determines the strength, ductility and wear resistance of the material acts as the synergistic characteristic. Currently, the probable methods of influence on the dislocation structure are an external electric field and an electric current.

2.6. Conclusion of Chapter 2

This chapter were examined the phenomena of generation of static electricity during the friction. Particularly, in detail were described the phenomenon electrification, tribo-electromotive and thermal electromotive force, also were given their objective laws. There were presented the processes of occurrence of significant electrical potential during friction bodies made of different materials. In the end of the chapter were examined several works about the influence of electric current on the wear during the friction processes.

3. The memristor

This chapter describes the memristor, the organization of its work, the mathematical and physical characteristics and also its properties.

3.1. Origin of the memristor

In accordance with the circuit theory it is known three basic two-terminal devices: resistor, capacitor and inductor. These elements are defined by the relation between two of the four fundamental circuit variables - current (i), voltage (v), charge (q) and flux (φ), where the time derivative of charge q is current i and according to Faradays laws voltage v is the time derivative of flux φ. Out of the *six* possible combinations of these four variables, five have led to well-known relationships. Two of these relationships are already given by [21]:

$$q(t) = \int_{-\infty}^{t} i(\tau) d\tau \tag{9}$$

and

$$\varphi(t) = \int_{-\infty}^{t} v(\tau) d\tau \tag{10}$$

Three other relationships are given, respectively, by the axiomatic definition of the three classical circuit elements, namely, the resistor is defined with the relation between the voltage v and current i as [21]:

$$dv = R \cdot di \tag{11}$$

The capacitor is defined with the relation between the charge q and voltage v as [21]:

$$dq = C \cdot dv \tag{12}$$

The inductor is defined with the relation between the flux φ and current i as [21] :

$$d\varphi = L \cdot di \tag{13}$$

Only one relationship remains uncertain, the relationship between φ and q. From the logical as well as axiomatic points of view, it is necessary for the sake of completeness to postulate the existence of a fourth basic two-terminal circuit element which is characterized by a φ-q curve [21].

The discovery of the existence of the fourth fundamental circuit element came to light in 1971 when Prof. Leon Chua proposed the missing relation between charge q and the flux φ through symmetry in Figure 11 [22]. Such an element can't be made from other base passive elements, although it can be modeled by a combination of active elements such as an operational amplifiers.

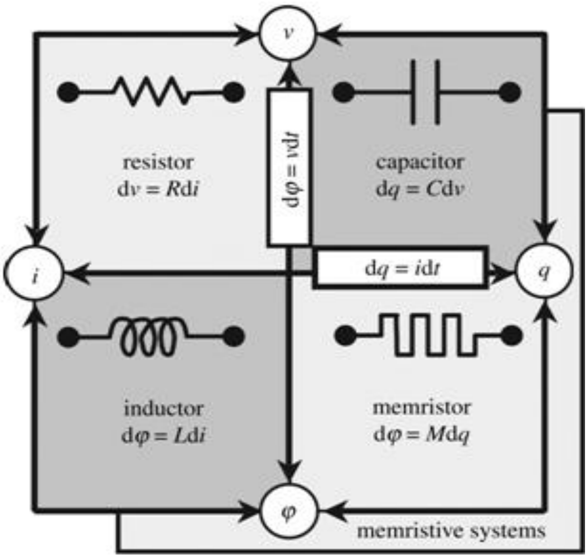

Figure 11 - The four fundamental two-terminal circuit elements : resistor, capacitor, inductor and memristor. Resistors and memristors are subsets of a more general class of dynamical devices, memristive systems. Note that R, C, L and M can be functions of the independent variable in their defining equations, yielding nonlinear elements. For example, a charge-controlled memristor is defined by a single-valued function M(q) [23]

Chua named the "missing" element the memristor - short from the words "resistance" and "memory". This name describes one of the characteristics of the memristor so-called hysteresis, the "memory effect", which means that the properties of this element depends on the applied prior force. In this case, the resistance of the memristor depends on the charge was passed therethrough, and that allows its use as a memory cell. This property was called memristance (M), whose value is the ratio of change of magnetic flux to change the charge. The value of the memristance depends on the amount of charge that has passed through the element, i.e. how long the electric current was flowed through this element.

The fundamental difference of the memristor from most types of newer semiconductor memory and its main advantage over them is that he does not keep its properties in the form of a charge. This means that the memristor is not afraid of the leakage of the charge and it is completely non-volatile. In other words, the data may be stored in the memristor for as long as there is material from which it is made. For comparison, the flash memory begins to lose the recorded information after years of storage without access to electric current. The theory was implemented in practice only in 2008, when developed the new appropriate materials and technology. The achieving the Hewlett Packard (HP) group of scientists led by Stanley Williams really is hard to overestimate: the first time since Faraday's times was able to physically reproduce a fundamentally new element of electrical circuits. The HP researchers, by fortunate coincidence, observed the memristive behavior of nanoscale cross-point devices in their crossbar memory arrays and credited the seminal work of Leon Chua published in 1970s to the nanoscale phenomenon they witnessed, that the entire electrical and computer engineering community was galvanized by the reemergence of the missing memristor as a fundamental circuit element since it kicked open new vistas in multiple frontiers ranging from the abstruse chaos theory to nanoscale commercial products [24].

3.2. Definition of the memristor

Memristor is a passive device that assigns the functional relation between electrical charge and magnetic flux. It is defined as a two terminal circuit element in which the flux between the two terminals is a function of the amount of electric charge that has passed through the device. A current-controlled time-invariant memristive system is represented as [25]:

$$\frac{dw}{dt} = f(w, i) \tag{14}$$

$$v(t) = R(w, i) \cdot i(t) \tag{15}$$

where w is an internal state variable, i(t) is the memristor current, and t is time. A memristor is a passive two-port device, with a varying resistance, depending on the total charge flowing through it. It behaves as a memory device, storing resistance as the memorized information [25].

Memristor is not an energy-storage element. Figure 12 shows the symbol for a memristor.

Figure 12 - Symbol of memristor [26]

The memristor is said to be charge-controlled if the relation between flux and charge is expressed as a function of electric charge q and it is said to be flux-controlled if the relation between flux and charge is expressed as a function of the flux linkage φ.

For a charge-controlled memristor [26]:

$$\varphi = f(q) \tag{16}$$

Differentiating equation (1) yields [26]:

$$\frac{d\varphi}{dt} = \frac{df(q)}{dq} \cdot \frac{dq}{dt} \tag{17}$$

We know that [26]:

$$v(t) = \frac{d\varphi}{dt} \tag{18}$$

$$i(t) = \frac{dq}{dt} \tag{19}$$

and

$$v(t) = M(q)i(t) \tag{20}$$

where [26]:

$$M(q) = \frac{df(q)}{dg} \tag{21}$$

$M(q)$ is called as memristance, and it has the units of resistance [26]. When the charge flows in one direction through a circuit, the resistance of the memristor increases, and its resistance decreases when the charge flows in the opposite direction in the circuit. If the applied voltage is turned off, thus stopping the flow of charge, the memristor - remembers the last resistance that it had. When the flow of charge is started again, the resistance of the circuit will be what it was when it was last active [27].

For a flux-controlled memristor [26]:

$$q = f(\varphi) \tag{22}$$

Differentiating equation (5) yields [26]:

$$\frac{dq}{dt} = \frac{df(\varphi)}{d\varphi} \cdot \frac{d\varphi}{dt} \tag{23}$$

We know that [26]:

$$i(t) = \frac{dq}{dt} \tag{24}$$

$$v(t) = \frac{d\varphi}{dt} \tag{25}$$

and [26]

$$i(t) = W(\varphi)v(t) \tag{26}$$

where [26]:

$$W(\varphi) = \frac{df(\varphi)}{d\varphi} \tag{27}$$

$W(\varphi)$ is called as memductance and it has the units of conductance [26].

3.3. Properties of the memristor

The memristor can be defined as a passive element circuit whose resistance is somewhat dependent on the charge passing through it. After switching off the voltage in the circuit, the memristor doesn't changes its state, i.e. it remembers the last resistance value.

Properties of the memristor can be demonstrated on the basis of a simple model. The impedance of the device in question can be represented as the sum of the resistances of the two variable resistors connected in series (see in Figure 13). One of the resistors (doped region) has a low resistance R_{on}, the other - a much higher resistance R_{off}.

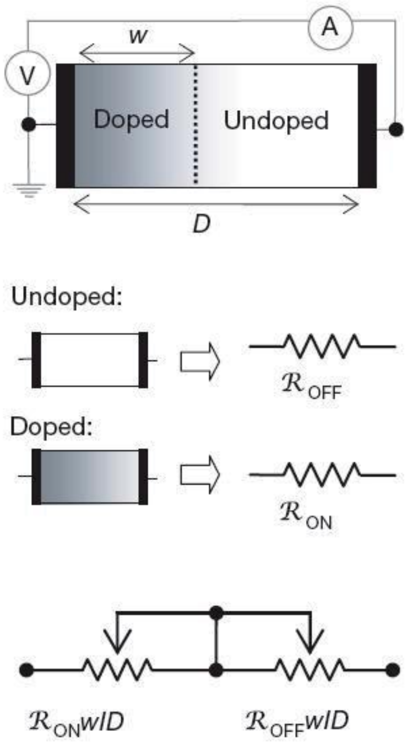

Figure 13 - Schematic diagram with the simplified equivalent circuit [23]

The memristor devices we are primarily concerned with are based on metal-oxides the device models considered here are based on the theoretical underpinnings proposed by Hewlett-Packard Labs. The basic premise is that charge transport in metaloxide memristors is based on a form of atomic rearrangement which adjusts the overall resistance of the device as a function of electric current [28]. For modeling purposes, a thin film metaloxide material of thickness D sandwiched between two conductors is modeled as two variable resistors connected in series, as shown in Figure 14. Each resistor in the model represents two distinct regions of the metal-oxide, one with a high ionic dopant concentration, R_{on}, and the other with a low concentration, R_{off} [29].

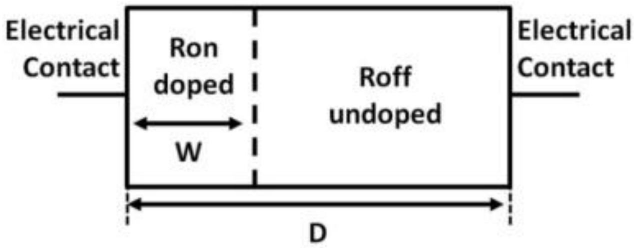

Figure 14 - Structure of the memristor [30]

When the voltage is applied on the metal contacts, ions begin to drift, and the border between the two regions is shifting. In this model, the relationship between current and voltage is given by [30]:

$$v(t) = \left(R_{ON} \frac{w(t)}{D} + R_{OFF} \left(1 - \frac{w(t)}{D} \right) \right) i(t) \tag{28}$$

At that the boundary is shifted according to the law [30]:

$$\frac{dw(t)}{dt} = \mu_V \frac{R_{ON}}{D} i(t) \tag{29}$$

where μ_V is the average ion mobility.

Upon integrating (29) we obtained the next expression for the width of the doped region [30]:

$$w(t) = \mu_V \frac{R_{ON}}{D} q(t) \tag{30}$$

For simplicity and ease of simulation the memristor resistance or memristance definition has been reduced to that of a current-controlled time-invariant one-port device given by [30]:

$$M(q) = R_{OFF} \left(1 - \ \mu_V \frac{R_{ON}}{D^2} \right) q(t) \tag{31}$$

where *w* represents the doped region of the memristor, D the total device length and R_{on}/R_{off} are the lowest and highest resistance states [23]. Thus, there can be different values for the memristance M as changes in the electric current cause atomic rearrangement and x is varied between 0 and D [30].

The two important conclusions are following from the expression (31). First, as predicted by Chua in his model, the resistance of the memristor is functions charge *q*, i.e. it depends up the total charge passing through the memristor. Secondly, the memristance increases sharply with decreasing D. Thus, the memristance becomes most important for the understanding of the characteristics of electronic devices as long as their dimensions are reduced to the nanometer scale.

If an alternating sinusoidal voltage of a certain frequency was applied to the memristor, its current-voltage characteristic takes the form reminiscent of Lissajous curve with center at the origin (shown in Figure 15). The memristor as distinguished from a resistor has hysteresis. With increasing frequency, voltage hysteresis curve degenerates into a straight line (see in Figure 15).

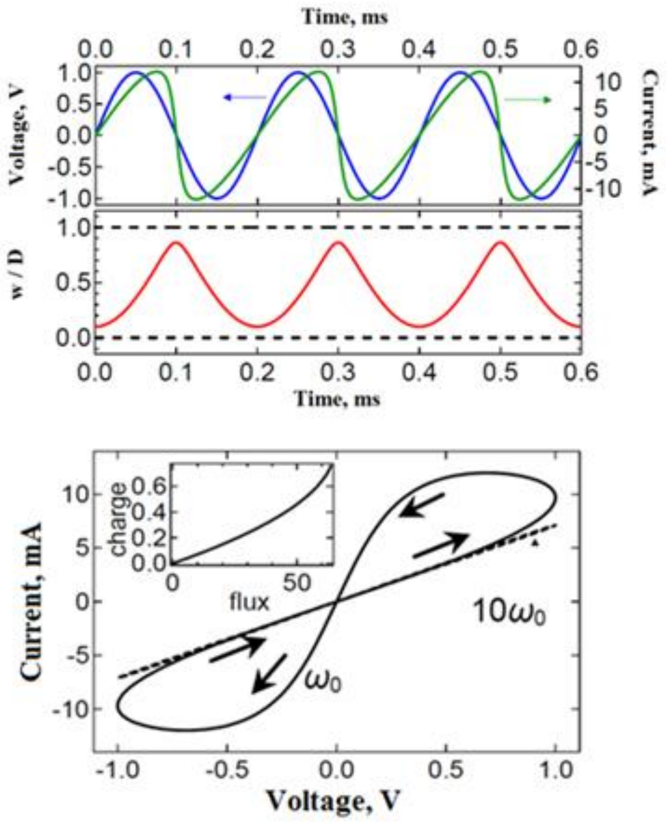

Figure 15 - Calculated memristor behavior under applied voltages and current-voltage characteristic of the memristor [23]

In real systems due to strong electric fields present in the nanoscale, demonstrate a strong non-linear effects in the transport of ions, and the curve of the current-voltage characteristic is changing. In the work [23] was described a similar volt-ammeter curve was obtained experimentally for memristor-based titanium dioxide (TiO_2), as shown in Figure 16.

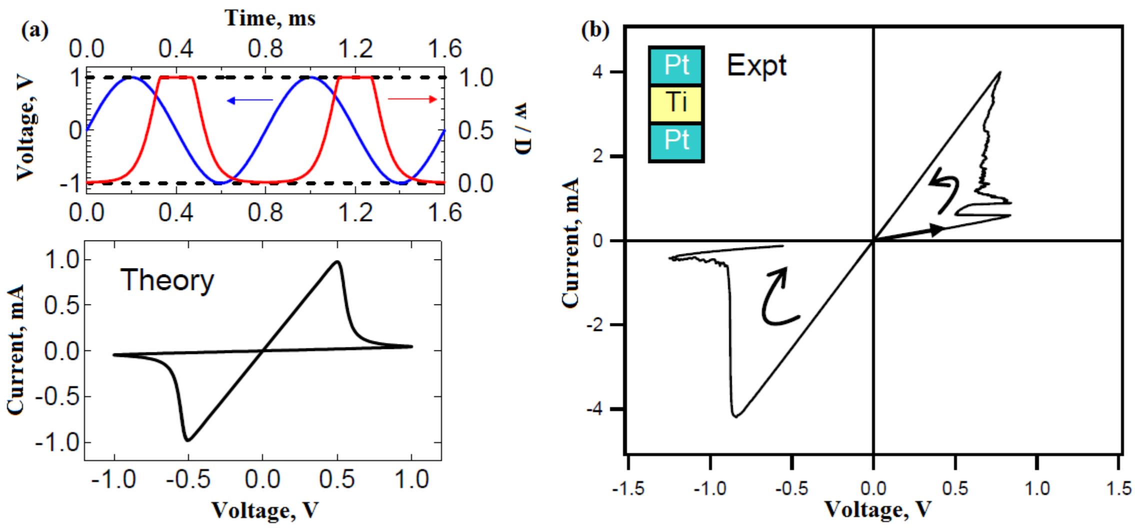

Figure 16 - The memristive switch: (a) simulation results and (b) experimental *i-v* curve [23]

This behavior of the memristor allows to use it as a bipolar switch: when voltage is applied to the opposite polarity, the memristor opens or closes an electronic circuit. If we consider the situation from the point of view of digital electronics, it can be said that the memristor changes its state from "0" to "1" and inversely. And this state of the memristor "remembers" and can be stored actually indefinitely - and for that end it doesn't require a voltage source. Currently, the time of the memristor switch from one state to another is of the order of 1 ns.

3.4. Operating peculiarities of the memristor

Structurally the memristor consists of a thin 50-nm film including two layers - the insulating layer of titanium dioxide and the layer oxygen depleted. The film is located between two platinum electrodes (thickness of 5 nm). When voltage is applied to the electrodes there is a change of the crystal structure of titanium dioxide: due to the oxygen diffusion the electrical resistance of the titanium dioxide increases by several orders of magnitude (thousandfold). In such a case, the changes in the cell are stored after shutdown of the current. Changing the polarity of the applied current switches the state of the cell, furthermore, according to HP, the number of such switching is not limited. In practice, the memristor can take not only the conventional two positions for a memory chips - either 0 or 1, and any value in the range from zero to one, so that such a switch is able to operate in both digital (discrete) and analog modes.

The view – Hewlett-Packard memristor has Crossbar type circuits comprise a grating of 40-50 nm wide by 2-3 nm thick platinum wires that are laid on top of one another perpendicular top to bottom and parallel of one another side to side. The top and bottom layer are separated by a switching element approximately 3-30 nm in thickness. The switching element contains of two equal layers of titanium dioxide (TiO_2). The layer interlaced to the bottom platinum wire is primary perfect TiO_2 and the other half is an oxygen deficient layer of TiO_2 constituted by TiO_{2-x} where x represents the quantity of oxygen deficiencies or vacancies. The whole circuit and mechanism can't be seen by the unaided eye and must be explored under a scanning tunneling microscope, as seen in Figure 17, in order to depicture the physical set up of the crossbar organization of the memristive circuit described in this section.

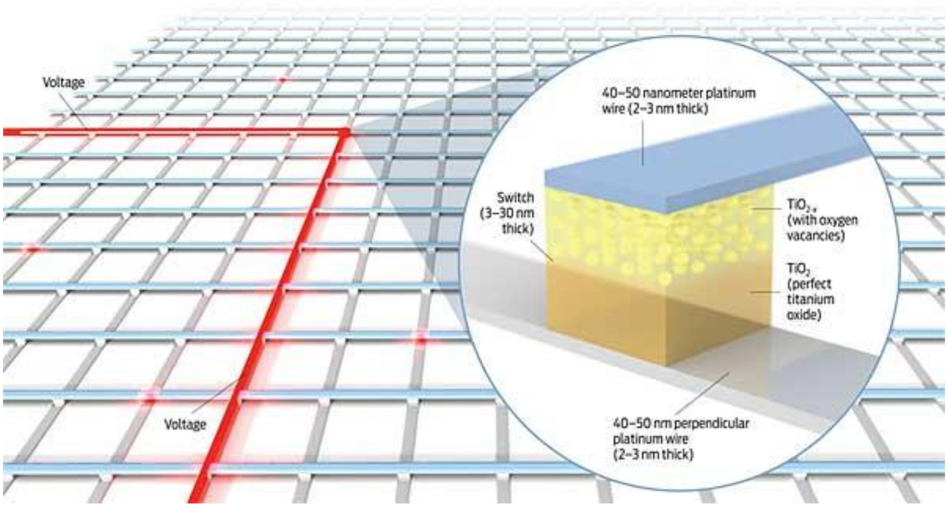

Figure 17 - Showing crossbar architecture and magnified memristive switch [31]

Actuation – the actuation of the memristor is switch and can be illustrated in three steps (see in Figure 18). The first of these steps is the application of power or more importantly current to the memristor. The second step composes of the number of time that the current flows across the crossbar gap and how the titanium cube transforms from a semi-conductor to a conductor. The third step is the actual memory of the cube that can be read as data.

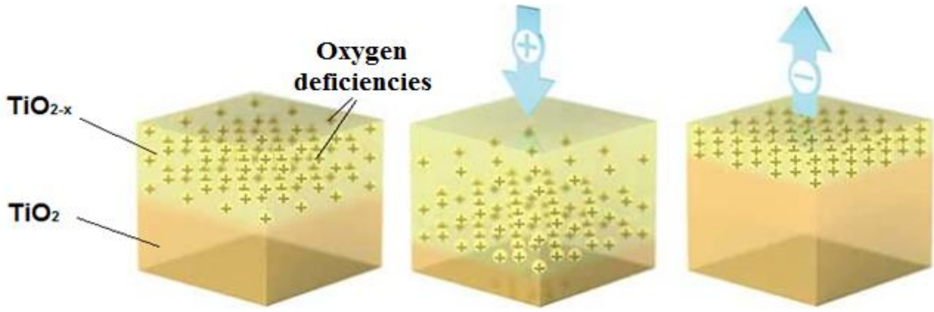

Figure 18 - Behavior of the memristor when positive and negative voltages are applied [31]

(a) TiO_{2-x} layer having oxygen deficiencies over insulating TiO_2 layer.

(b) When a positive voltage is applied, the positively charged oxygen vacancies in the TiO_{2-x} layer are repelled, moving them towards the undoped TiO_2 layer. As a result, the boundary between the two materials moves, causing an increase in the percentage of the conducting TiO_{2-x} layer. This increases the conductivity of the whole device.

(c) When a negative voltage is applied, the positively charged oxygen vacancies are attracted, pulling them out of TiO_2 layer. This increases the amount of insulating TiO_2, thus increasing the resistivity of the whole device.

When the voltage is turned off, the oxygen vacancies do not move. The boundary between the two titanium dioxide layers is frozen.

Step 1 – as aforesaid, each gap that combines the two platinum wires composes a mixture of two titanium oxide layers. The initial state of the combination is half-way between conductance and semi-conductance. Two wires are selected to apply power to in either a positive or negative direction. A positive direction will endeavour to close the switch and a negative direction will try to open the switch. The application of this power will be able to completely open the circuit between the wires but it will not be able to completely close the circuit since the material is still a semi-conductor by nature. Power can be selectively placed on certain wires to open and close the switches in the memristor.

Step 2 – the second step includes a process that takes place at the atom level and is not visible by any means. It includes the atomic action that the gap material, made from titanium dioxide, goes through that opens and closes the switch. The initial state of the gap is neutral meaning that it contains of one half of pure titanium dioxide TiO_2 and one half of oxygen starved titanium dioxide TiO_{2-x} where x in the initial state is 0.05. As positive current is applied, the positively charged oxygen vacancies push their way into the pure TiO_2 causing the resistance in the gap material to drop, becoming more conductive, and the current to rise. Inversely, as a negative current is applied the oxygen vacancies withdraw from the pure TiO_2 and condense in the TiO_{2-x} half of the gap material causing the pure and more resistive TiO_2 to have a greater ratio slowing the current in the circuit. When the current is raised the switch is considered open (HI) and for data purposes a binary 1. As current is reversed and the current is dropped the switch is considered closed (LOW) or a binary 0 for data purposes.

Step 3 – third step interprets the final step of the memristance change and is the actual step that makes the circuit memristive in nature. As indicated earlier, the concept of memristor is a resistor which can remember what current passed through it. When power is no longer applied to the circuit switches, the oxygen vacancies remain in the position that they were last before the power was shut down. This means that the value of the resistance of the material gap will remain until indefinitely until power is applied again. This is the true meaning of memristance. With an insignificant test voltage, one that won't affect the movement of molecules in the material gap will allow the state of the switches to be read as data. This means that the memristor circuits are in fact storing data physically. If we want a positive voltage to turn the memristor off, then we want the titanium oxide layer with vacancies on the top layer. But if you want a positive voltage to turn the memristor on, then you need the layers reversed. In its initial state, a crossbar memory has only open switches, and no information is stored. But once you start closing switches, you can store vast amounts of information compactly and efficiently [32].

3.5. Conclusion of Chapter 3

In this chapter were discussed the main parameters of the memristor, its properties and working theory.

4. Modeling of the memristor

This chapter describes the physical principles of the memristor based on metal oxides (for three different tipes: the model of the HP memristor, the memristor model based on TiO_2 and the memristor model based on the three-component oxide $HfAlO_x$). Also in this chapter was describes the creation of the memristor model in environment MatLab/Simulink.

4.1. Review of materials used in the manufacture of a memristor

For the first time ever the memristance effect has been experimentally demonstrated in 2008 for a system of metal-insulator-metal (Pt-TiO_2-TiO_{2n-1}-Pt). There was demonstrated that the memristance effect occurs in nanoscale metal-insulator-metal structures due to the movement of charges in the hyperfine dielectric layer upon application of an electric field, for example, during the motion of oxygen vacancies in the layer of titanium dioxide. In recent years, there are proposed a number of alternative materials for use as the active layer of a memristor.

The memristance effect was demonstrated in the nanopore-ion solution, in the devices based on the current-conducting polymers and the protein molecules, the nanoparticle assemblies, in particular, nanoparticles of the monocrystalline magnetite (Fe_3O_4). However, the memristors based on such materials are formed by methods not characteristic of the modern technology of the silicon integrated circuits. Accordingly, the use of these materials as the active layer of the memristor makes it difficult for integration of the memristor into the modern production. Therefore, as a basis of the memristor-electronic devices, there is most commonly using metal-insulator-metal, which easily integrated into silicon technology. As in the first manufactured memristor, as the dielectric layer commonly used titanium oxide TiO_2-Ti_nO_{2n-1} thickness of 5-40 nm, as well as other metal oxides: ZrO_2-ZrO_{2-x}, HfO_2-HfO_{2-x}, VO_2-$VnO_{2n-1,}$ Nb_2O_5-NbO_2, Ta_2O_5-TaO_2, MoO_3-Mo_nO_{3n-1}, Fe_2O_3-Fe_3O_4, Ni_2O_3-Ni_3O_4, Co_2O_3-Co_3O_4. One approach to improve the functional properties of the memristor based on transition metal oxides (TiO2, HfO2, ZrO2) is the alloying of oxide by dint of the trivalent dopant, for example, aluminium. There are theoretical work, which shows that the addition of Al in ZrO_2 reduces the energy of formation of oxygen vacancies about 1.7 times, whose motion in the electric field provides ultimately the memristance effect of the structure [33].

4.2. Physical principles of the memristor based on metal oxides

The reversible effect of conductivity change of the memristor called the resistive switching effect. As the memristors and other structures with the resistive switching effect most commonly used the metal-dielectric-metal structures (MDM). The effect of the resistive switching MDM-structure to be as follows: there is the change in the dielectric conductivity by up to several orders of magnitude under the influence of an electric field generated in the insulator (shown in Figure 19).

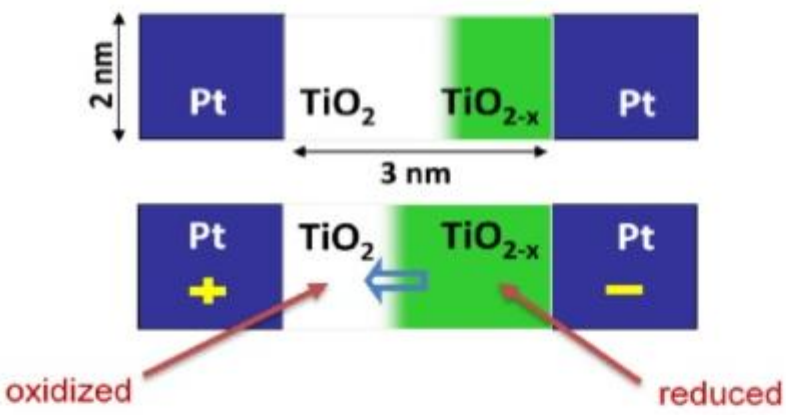

Figure 19 - The effect of the resistive switching MDM-structure [34]

There are several generally accepted of the resistive switching mechanisms and, accordingly, types of the memristors. The most common type of the memristor - the type, where resistive effect is caused by the reaction of reduction/oxidation of the oxide is used as the dielectric of the memristor MDM-structure. Drift of the oxygen ions and the vacancies of oxygen in the depth of the oxide layer accompanies the reaction reduction / oxidation oxide. The oxygen vacancies serves as the traps for electrons, which transferred the charge from one metal electrode to the other. Depending on the concentration of oxygen vacancies and their distribution in the oxide MDM-structure can be in a high-impedance (high resistance state - HRS), or a low-resistance state (low resistance state -

LRS). There is be able to monitor the concentration of oxygen vacancies in the oxide layer in order to achieve a stable of the resistive switching effect.

By now, for such a transition metal oxide as a HfO_2, ZrO_2, TiO_2, Ta_2O_5, NiO demonstrates the effect of reversible resistive switching, which consists in changing the dielectric conductivity by up to several orders of magnitude when a voltage amplitude is a definitively stated (unipolar switching), and in some cases at a certain amplitude, but subject to change polarity (bipolar switching) [35].

4.3. Choice of a modelling environment

There are many different environments of the applications of mathematical programs, which provides an open environment for engineering (technical) and scientific computing, as well as to build models. The main and most common of these are: MatLab, GNU Octave, FreeMat, Maxima and Scilab [36].

In the course of operation, it was decided to use a multi-paradigm numerical computing environment MatLab (matrix laboratory). This environment is the most common, it runs on most modern operating systems, it has a user-friendly graphical interface and easy to use. However, there are minor drawbacks: high cost of licenses and incomplete support of statistical functions.

During the process of the create a model of the memristor was used the program Simulink, which is a supplement to the package MatLab. In the simulation with using Simulink was implemented the visual programming principle in accordance with which the user on the screen of the library of standard blocks and creates a device model performs calculations. One of the major advantages of the program - a test of the results in real time. Ability to set in blocks of any mathematical expressions can solve both routine tasks and try new solutions and finding the most effective compromises. It is also very important economic factor - the use of the program reduces the need to purchase samples and reduces the cost of testing. This package contains an extensive library of components of the block diagram, as well as user-friendly editor components.

This program was chosen because in contrast to the classical ways of modeling, the user does not need to thoroughly study the language of mathematics and numerical methods, and enough general knowledge required when working on the computer and, of course, knowledge of the subject area in which it operates. When you work with Simulink the user has the ability to upgrade the library blocks, create your own, and make new library blocks. In the simulation, the user can select the method for solving differential equations, as well as a way of changing the model of time (with a fixed or variable pitch). During the simulation it is possible to monitor the processes occurring in the system. To do this, there is using special surveillance devices that are part of the library Simulink. The simulation results may be presented as graphs or tables [37].

4.4. Create of the memristor model in environment MatLab/Simulink

During the process of modeling, it was based on the memristor model proposed by student Thang Hoang from Hanoi University of Science and Technology [38]. This model simulates the mathematical characteristics of the memristor to the full extent. But for a more detailed study of the electrical characteristics of the memristor, it were made some adjustments in the circuit, videlicet, added output M (memristance) in the sub-model of the memristor. This output is modelling of the change of the memristor resistance over time.

The constructed model is presented in Figure 20.

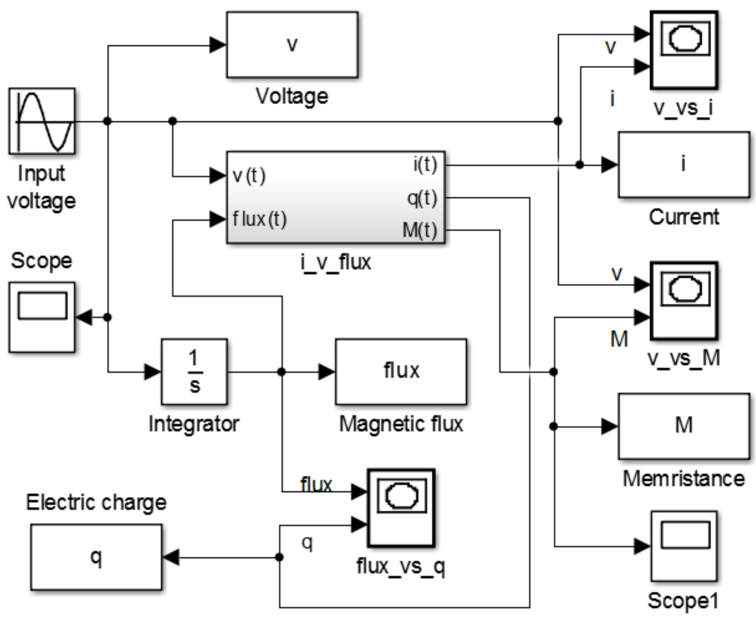

Figure 20 - The memristor model

In this model, the block "Input voltage" generates (as the name implies) the input voltage. The diagram of the input voltage change and its parameters are shown in Figure 21 and Table 1, respectively.

The blocks "Scope" and "Scope1" show the graphs of the change of the input voltage and of the memristance in a time. The blocks "Voltage", "Current", "Magnetic flux", "Memristance" and "Electric charge" record the values of the electrical parameters and transfer them as a vector in the environment MatLab. The other blocks ("v_vs_i", "v_vs_M" and "flux_vs_q") construct of the dependency diagrams, which will be shown later.

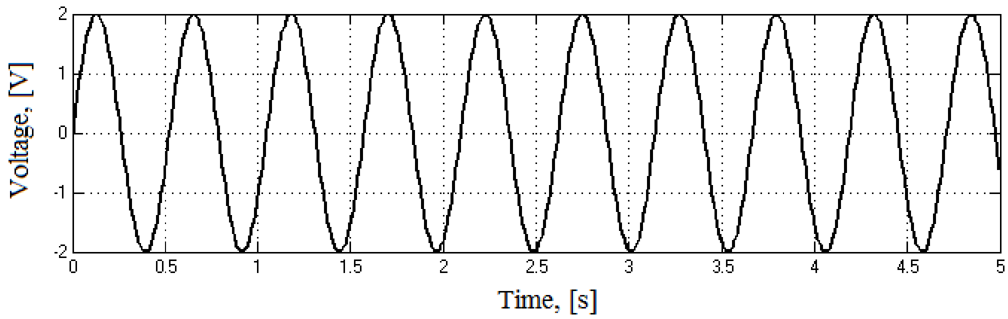

Figure 21 - The input voltage change

Table 1 - Parameters of the input voltage

Name title	Magnitude
Amplitude	2
Frequency	1,875 [Hz]

The values of these parameters (amplitude and frequency) were chosen taking into account the dimension of the value of electrical characteristics the tribocontact (described below). If the settings is changed, the dependence of the electrical characteristics of the memristor would have a different character. Increasing the amplitude and frequency of the input voltage will be directly proportional on the values of the memristor (drop in voltage, current, and memristance) i.e. the graph of the dependence of voltage vs current and voltage vs memristance will stretch along the axes.

Subsystem i_v_flux (shown in Figure 22) simulates the electrical processes in the memristor. During the construction of the sub-models we used all memristor mathematical functions presented above (equations 28 - 31). As the input parameters were used the voltage and the magnetic flux, as output - the current, the electric charge and the memristance. Also the model contains 5 blocks, which modeling the memristor parameters: R_OFF - the off-state resistance; R_ON - the on-state resistance; D - the thickness of the memristor film; w_0 - the length of the doped region; Muy_D - the average ion mobility. The block "Nuy" contains the value numerical value of the amount of substance for the memristor material.

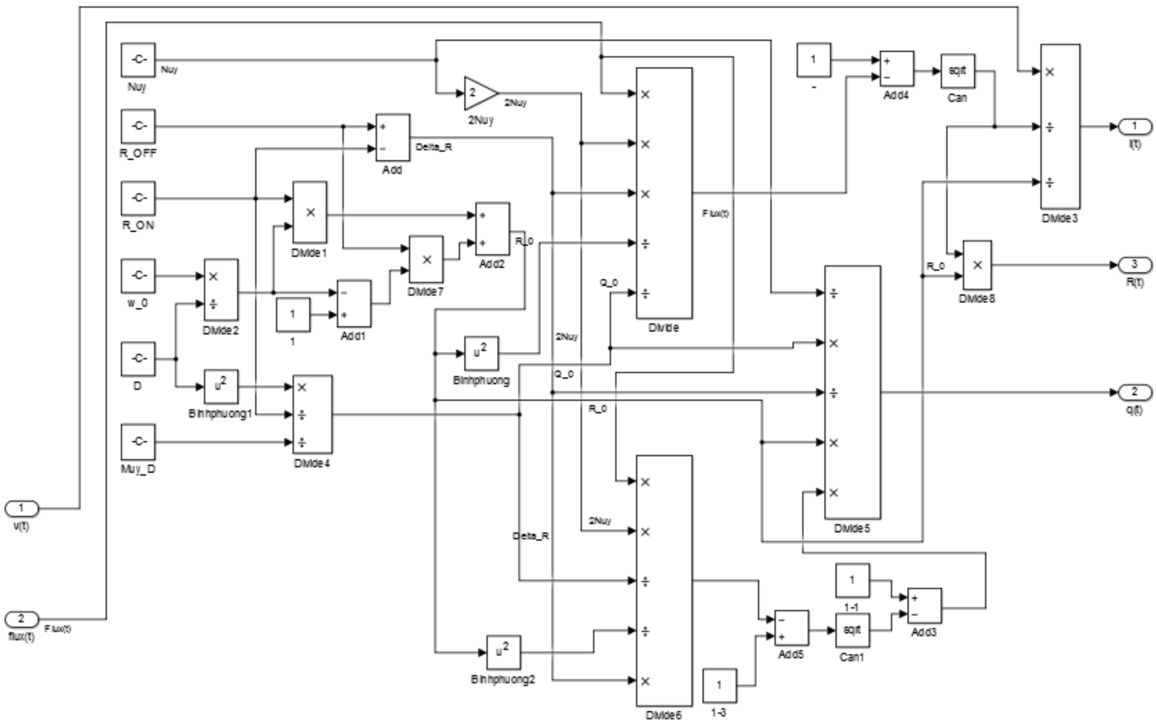

Figure 22 - The memristor model in MatLab/Simulink environment

For a more detailed study of the characteristics of the parameters were used the different memristor models. There was also used the parameters of the real memristor was created by the Hewlett-Packard company. These memristors have different manufacturing process and the materials of which have been made.

4.5. Model of the HP memristor

In 2008, researchers at HP, led by Stanley Williams built a working prototype of a memristor (it was named the crossbar system, which shown in Figure 23), there is placed a microscopic film of titanium dioxide between the two platinum electrodes, one of which has been oxidized.

The memristor was fabricated as follows:

- they sandwiched a cube of TiO_2 between platinum crossbars;
- a region of the TiO_2 was auto doped by removing oxygen atoms creating a TiO_{2-x} region;
- these positive oxygen deficiencies can drift through the entire cube and are moved by applying an electric current;
- this movement changes the resistance of the memristor;
- the dopants will also remain in their position until a current is applied again. In this way the memristor has memory.

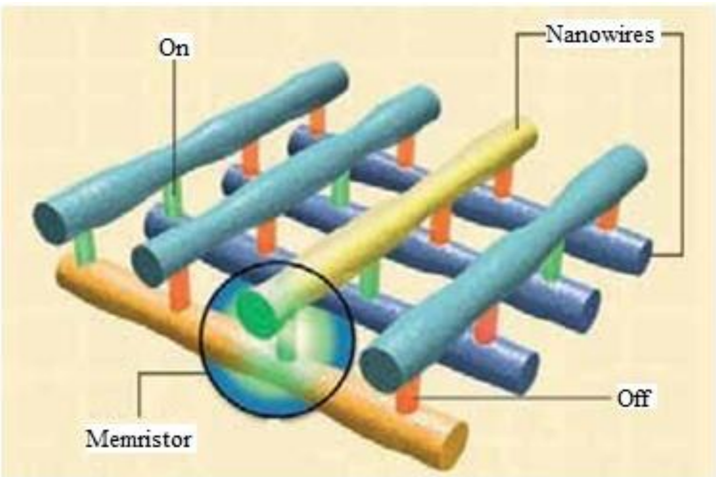

Figure 23 - The crossbar system [30]

The mathematical description of the memristor was given in Chapter 3. Features of the memristor are presented in Table 2.

Table 2 - Characteristic of the HP memristor

Name title	Magnitude
thickness of the memristor film	D =10 [nm]
average ion mobility	$\mu_v = 10^{-14}$ [$m^2 s^{-1} V^{-1}$]
on-state resistance	R_{ON} = 100 [Ω]
off-state resistance	R_{OFF} = 10 [kΩ]

Finally, using the characteristics of the HP-memristor for the model, there were built the dependency diagrams: voltage vs current, magnetic flux vs charge, voltage vs memristance, and change of memristance (shown in Figure 24).

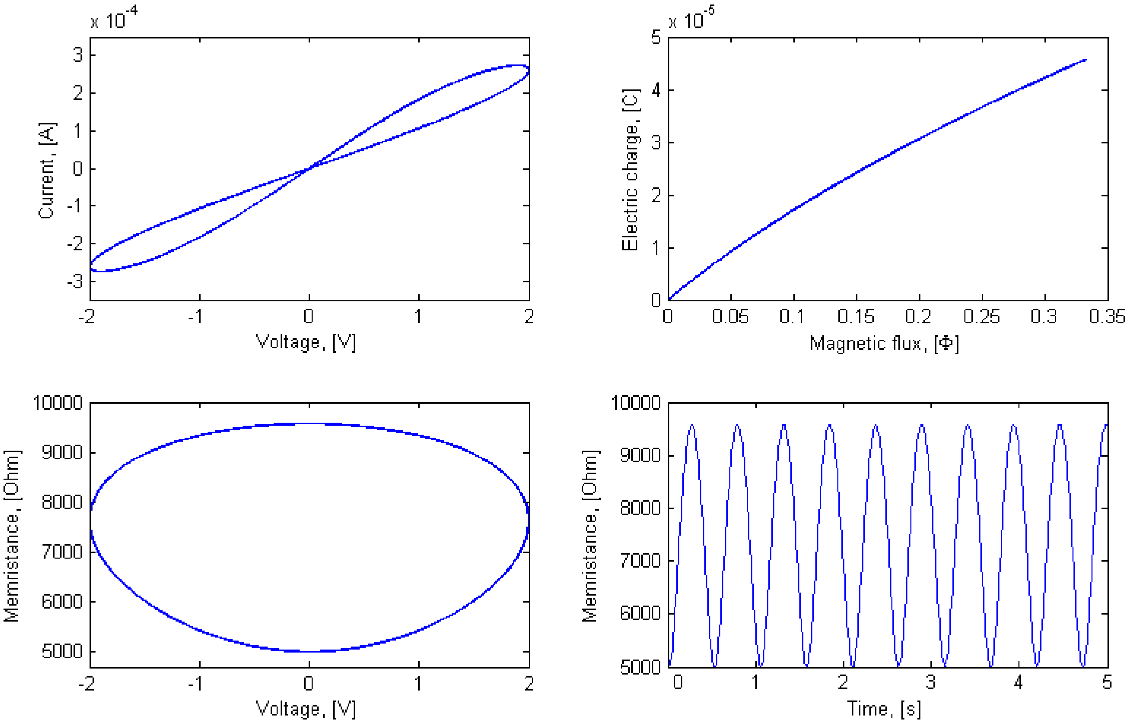

Figure 24 - The dependency diagrams of the HP-memristor

These results allow us to see the main characteristics of the memristor such as hysteresis loop of electrical parameters (volt-ampere characteristic). It means that current value depends up previous state.

Analysis of the dependency diagrams the voltage vs current and the voltage vs memristance allows us to conclude that the electrical characteristics of the memristor, in particular the current, voltage and memristance depend on the prehistory of changing parameters, i.e. the current value of the variable depends up the previous value. Such conclusions can be drawn for the other two types of the memristors are shown farther.

4.6. Investigation of the memristor model based on TiO_2 with different characteristics

In the work [39] was investigated the effect of structural parameters of the memristor based on titanium oxide on its electrical characteristics. To study, there were prepared the structures consisting of two layers - a layer of titanium oxide depleted TiO_x (x=1,6) and a layer of titanium dioxide TiO_2 - located between two platinum electrodes. Creation of the memristor specimen was produced by approach of pulsed laser deposition using a solid target of titanium dioxide TiO_2 and platinum Pt. The layer thickness of titanium dioxide and depleted of titanium oxide, which had range from 3 to 30 nm for the layer of TiO_2 and from 10 to 60 nm for the layer TiO_x, served as the structural parameters memristors.

The investigation of the electrical characteristics of the memristor was conducted by measuring their current-voltage characteristics and the dependence of the resistance of the element on the number of switching cycles, obtained with the use of a signal analyzer and a probe station. The studies have shown that the best performance among the examined samples memristors have the following structural parameters: 1) the thickness of TiO_2 - 20 nm thickness TiO_x - 40 nm; 2) the thickness of TiO_2 - 30 nm thickness TiO_x - 30 nm. These samples have a higher resistance to the cycling process, in particular, their cycling resistance at least 2 times higher compared with the other examples. Also, these samples have a large difference between the maximum and the minimum value of the resistance element, namely the ratio of the maximum to the minimum value of resistance of these samples is on average about 80-100. In addition to the above, the value of the voltage switching for all samples are comparable in magnitude and have the average of voltage value 2-3 V. The estimated dependency diagrams for these memristor models are shown in Figure 25.

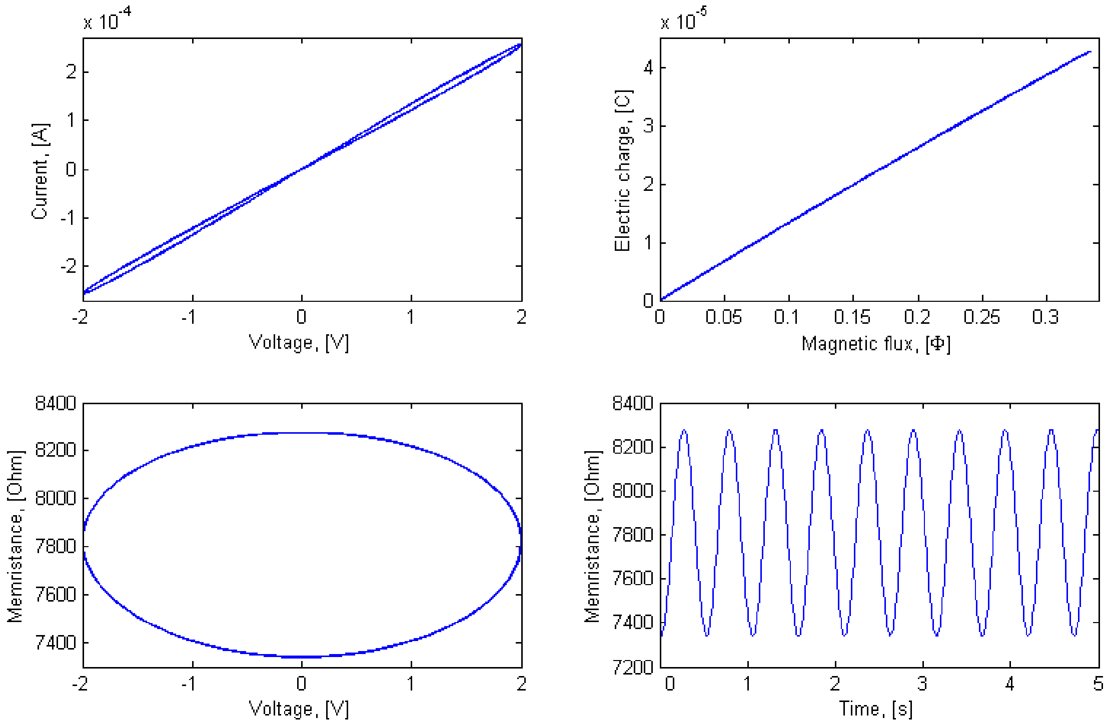

Figure 25 - The dependency diagrams of the memristor based on TiO_2

It may be noted that this type of memristor also has a hysteresis loop of electrical parameters, but the diagram of the dependency voltage vs current more like a straight line, this indicates that this type of behavior of electrical parameters of the memristor is similar of a linear resistor.

4.7. Investigation of the memristor model based on the three-component oxide $HfAlO_x$

The sample of the memristor is made on silicon substrates and represents the MDM-structure (see in Figure 26).

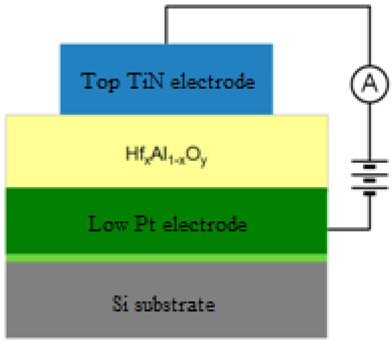

Figure 26 - The memristor model based on the three-component oxide $HfAlO_x$ [40]

The lower electrode is a metal layer Pt with a underlayer Cr, deposited on the whole area of the substrate. The thickness of the Pt layer was 50 nm, the thickness of Cr layer was about 10 nm. the three-component metal oxide $Hf_xA1_{1-x}O_y$ has the thickness 6-10 nm and was spreaded on the entire area of the substrate. The upper electrodes consist of the metallic TiN layer thickness of 50 nm and Al layer having a thickness of 100 nm. The electrodes were deposited through a shadow mask with a hole diameter of 50-750 microns and they are the separately located contacts [40].

The parameters and the estimated dependency diagrams for the memristor model are shown in Table 3 and in Figure 27 respectively.

Table 3 - Parameters of the memristor based on the three-component oxide $HfAlO_x$

Name title	Magnitude
thickness of the memristor film	D = 120 [nm]
average ion mobility	$\mu_v = 12 \cdot 10^{-13}$ [$m^2 s^{-1} V^{-1}$]
on-state resistance	R_{ON} = 100 [Ω]
off-state resistance	R_{OFF} = 10 [kΩ]

This type of memristor is the most interesting to study because the law of change the electrical characteristics somewhat different from previous types of memristor. Memristance of this type is more subtle depends on the voltage change than others memristor.

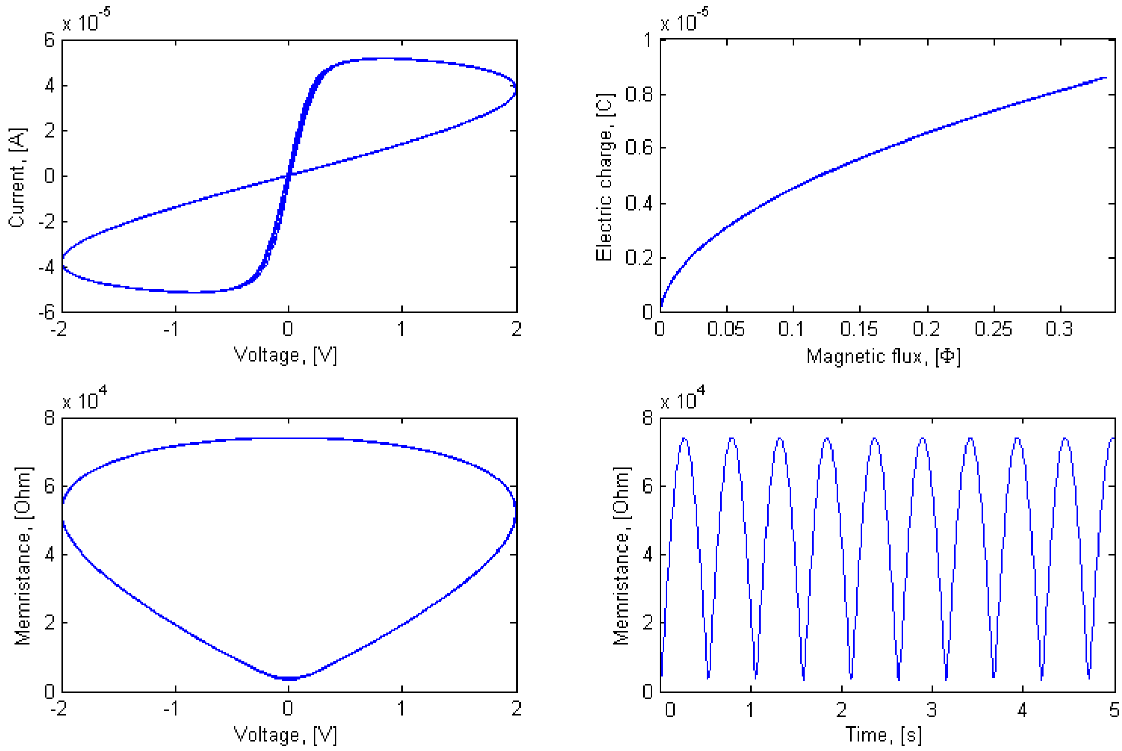

Figure 27 - The dependency diagrams of the memristor based on $HfAlO_x$

4.8. Conclusion of Chapter 4

In this chapter was conducted review of materials used in the manufacture of a memristor, was created of the memristor model in environment MatLab / Simulink, was built the graphs of change regularity of the electrical characteristics for different types of memristors.

As expected, the change in the parameters (for example, such as the off-state resistance, the on-state resistance, the thickness of the memristor film) and / or material of the memristor is fundamentally affects the appearance of the dependency diagrams of the voltage, current, memristance, magnetic flux and electric charge.

5. Investigation of friction processes

This chapter describes the conducted tribological experiments. Here was given the review of the equipment whereby the tests were conducted, also here was described the processes of friction occurring in the course of the experiments. The chapter describes the use of the package System Identification Toolbox for searching the transfer function, which describes the relationship between the electrical resistance of contact tribopair and resistance of the memristor.

5.1. Review of the device for study of friction processes

To study the tribological characteristics was used the Tribometer of German company WAZAU. The tribometer (shown in Figure 28) serves for the investigation and simulation of friction and wear processes under sliding conditions. It can be operated for solid state friction without lubrication and for boundary lubrication with liquid lubricants.

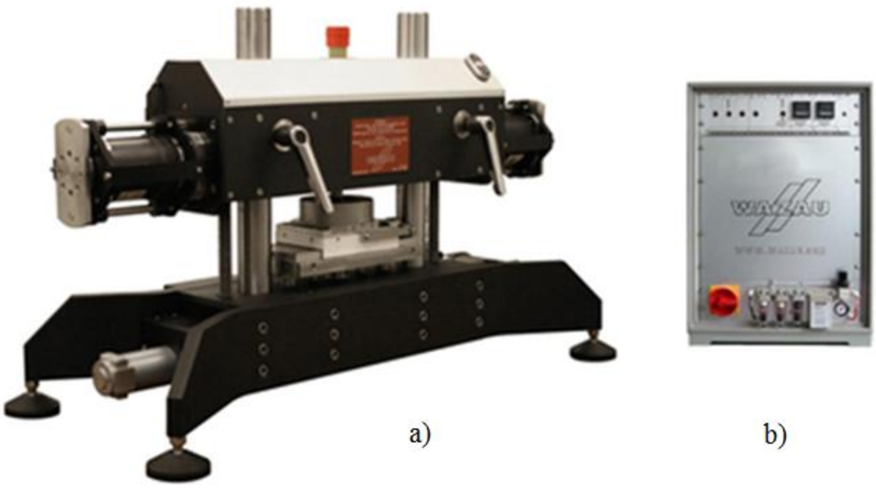

Figure 28 - Appearance of the tribometer: a) test rig; b) control rack [41]

According to the standard test principle a stationary test specimen (pin or disc) with a defined normal force is pressed against the surface of a rotary disc. Both specimens are perpendicularly arranged one on the other whereby the rotary disc is on top. Other test configurations are possible. The normal force is applied by the movable drive block and the drive spindle. The normal force is damped by means of a spring located below the linear table. The tribometer is driven by a servo motor steplessly adjustable from 0.1 rpm to 3000 rpm.

The actual test equipment essentially consists of the motor unit, the drive and the load section. The shift able modules are one on the other fastened to two perpendicularly columns. Pin and disc are in a specimen pot heat able up to approximate 150 °C. During the test the normal force, the temperature inside the pot, the linear wear amount of both specimens and the friction torque are continuously measured.

The measurement of the normal force is done by a force sensor arranged between counter load spring and lower specimen restraint. The temperature is measured by a NiCr-Ni-thermocouple in the pot. The wear is measured over the changing displacement between lower and upper specimen restraint. The measurement is done contactlessly by a laser-optical displacement sensor. The friction torque is measured by a rotary torque sensor.

All measuring signals are transferred to the control rack to be conditioned there. Data acquisition is done by an USB measuring module with a solution of 16 bit. The measured values of rotational speed and temperature are digitally monitored with temperature values sampled at 2 Hz and rotational speed sampled at 5 Hz [41].

5.2. Description of the friction process

In this work, we carried out the study of friction under the tribological scheme ball on plate. In the role of a friction is understood a resistance which takes place when moving one body relative to another, which is pressed against the first. There are difference between the static friction and the sliding friction (see in Figure 29).

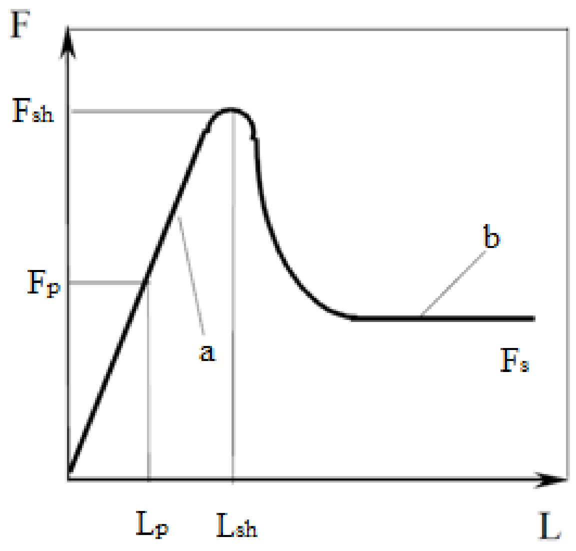

Figure 29 - Typical cases of the formation of frictional forces: a) the force of static friction; b) the sliding frictional force [42]

The force of static friction (F_p) is called a shear load applied to the contacting bodies and it don't cause their mutual sliding (see in Figure 1(a)). In such case this relative movement (L_p) is achieved by deformation of the material of the roughness in the contact zone and is called the preliminary displacement. Essentially, it has a elastic character and disappear when removing the shear load. However, progressively as the increase of the shear load, the displacement takes the plastically character and becomes partly irreversible. In Figure 1 shown the maximum amount of the preliminary displacement (L_{sh}) and respectively, the limiting value of the forces of static friction, which is called the static friction force. With further increase of the sliding the movement starts.

The frictional force can be represented as a product of the specific friction force (τ) and the actual contact area (A_r) [42]:

$$F = \tau \cdot A_r \tag{32}$$

Friction coefficient be represented as the ratio of the friction force to the normal force acting on a contact [42]:

$$\mu = F/N \tag{33}$$

There are also distinction of the coefficients of static friction (static) and sliding (kinetic).

Depending on the nature of the lubricant layer there are 4 kinds of friction: dry friction, boundary friction, hydrodynamic (liquid) friction and mixed (simultaneous there are components are dry, boundary and hydrodynamic friction). In the first case, there are contacted non-lubricated the surfaces, which coated with oxide films and the subtlest layers of gases and water molecules, which was adsorbed from the environment (this kind of friction and has been used in this work). In the second case, in addition to these films, lubricant molecules are present in the form of a thin layer of a few molecules thickness, which is firmly connected to the surface. In the third case, a layer of liquid lubricant completely separates the mating surfaces.

The dry friction and the boundary friction are similar in nature and have common patterns. The reason is the fact that during the process of the boundary friction mono molecular layers of lubricant is firmly bound to a solid surface, have solid properties and they serve like as the continuation of the solid phase. Therefore, as in the dry frictional, actually the contact occurs two solid surfaces. The difference manifests itself in the different values of the coefficient of friction. If the friction coefficient for dry friction is usually greater than 0.2, then in process of the boundary friction of its value be in the range of 0.05-0.2.

The mechanism of friction is explained the molecular-mechanical theory of friction, on the development of which contributed greatly to the Russian scientists (B.V. Derjaguin, I.V. Kragelsky etc.). According to this theory, the friction has a dual molecular-mechanical nature. The frictional force can be represented as the sum of the molecular (adhesion) constituent and the mechanical (deformation) constituent [42]:

$$F = F_A + F_\Delta \qquad (34)$$

Molecular component leads to the rupture of molecular or atomic bonds that occur between the contacting bodies. The mechanism of this process is similar to the destruction of the crystal lattice during the process of shear. The scattering of the friction work due to heat occurs due to the elastic deformation of the crystal lattices. The work of the external force is changing into the potential energy of grids. After disconnection of the linking, the potential energy is converted into vibrational energy of atoms - to the internal. After disconnection of the linking, the potential energy is converted into the vibrational energy of atoms - to the internal [42].

5.3. Description of the experiments

The experiments for the study of friction were conducted using tribometer (which was described above). As specimens were used the deposited coating TiN and AlTiN materials. These materials are the most relevant and widely used as coatings for cutting tools. The study of the characteristics of materials will help to better understand the features of occurrence of electrical phenomena in the process of friction, which in turn have an impact on the wear and on other tribological characteristics.

The scheme of friction process is reciprocating movement ball on plate. The experimental conditions are presented in Table 4. The record of results was carried out with a frequency of 0.01 Hz.

Table 4 - The experimental conditions

Name title	Magnitude	
Friction pair	Al_2O_3 - TiN	Al_2O_3 - AlTiN
Movement amplitude	0.01 m	
Frequency	5 Hz	
Normal force	22 N	
Top specimen - ball		
Diameter	0.01 m	
Material	AL_2O_3	
Lower specimen №1 - plate		
Material of the plate base	42CrMo4	
Material of the deposited coating	TiN	
Lower specimen №2 - plate		
Material of the plate base	42CrMo4	
Material of the deposited coating	AlTiN	

During the experiment the different characteristics of friction pair were recorded: the normal force, friction force, coefficient of friction, wear, etc (shown in Figure 30 and Figure 31 for friction pairs Al_2O_3 - TiN and Al_2O_3 - AlTiN respectively).

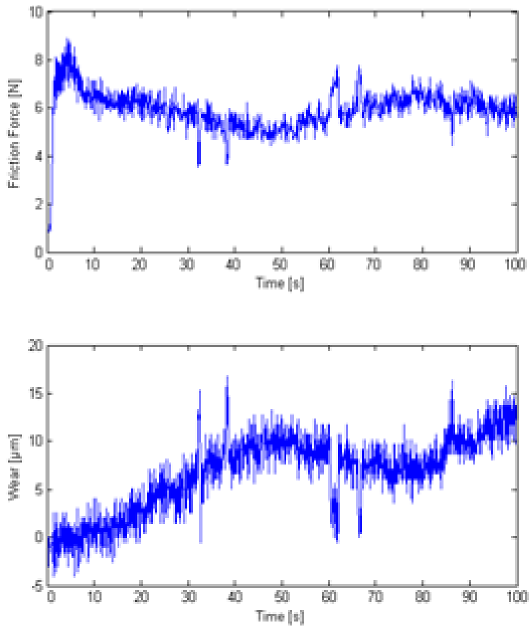

Figure 30 - Some of the experimental data from the tribometer (results for friction pair Al_2O_3 - TiN)

But of special interest is the change of electrical resistance of contact friction pairs (which can be seen in Figure 30 and Figure 31 as dependency diagrams of the contact resistance vs the time).

It is this relationship allows you to find the relationship between the electrical characteristics of the tribopair contact and the electrical characteristics of the memristor.

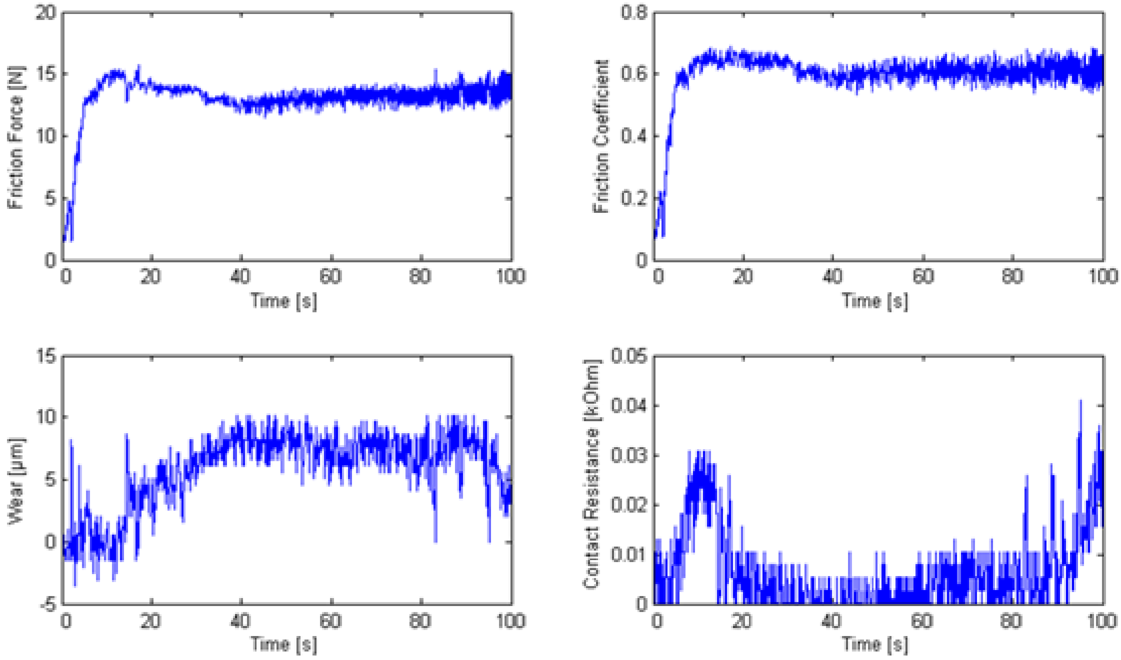

Figure 31 - Some of the experimental data from the tribometer (results for friction pair Al_2O_3 - AlTiN)

5.4. System Identification Toolbox: obtaining of the transfer function

System Identification Toolbox provides capabilities for building mathematical models of dynamic systems from measured input and output data of the real system.

System Identification Toolbox provides the functions MATLAB, Simulink blocks and interactive tools to create and use models of dynamic systems. It is possible to use the data input, output in time and frequency domain for identification of continuous and discrete transfer function, models of the processes and state-space models.

With the help of the System Identification Toolbox can use the following methods of identification:

- maximum likelihood;
- minimization of the prediction error (PEM - prediction-error minimization);
- identifying a subset of the system;
- other methods of identification.

For a nonlinear system dynamics can be assessed the models of Hammerstein-Wiener (Hammerstein-Weiner) and nonlinear models ARX (AutoRegresive model with eXternal input) with the wavelet network, the model with a tree and the models with nonlinear sigmoidal network.

With the help of the System Identification Toolbox can be used to identify the system as a black box for the estimation of the parameters defined by the user model. You can use the identification model to predict the response of the system and for the simulation in Simulink.

System Identification Toolbox allows the user to simulate the time sequence data and perform forecasting of temporal sequence.

System Identification Toolbox allows the user to model the measured data input and output. With it you can:

- to analyze and process the data;
- to identify the suitable structure, the model order and perform an assessment of the model parameters;
- check the validity of the resulting model.

You can use identified linear models for the analysis and design of control systems using the Control System Toolbox. You can add Identified in Simulink models using blocks provided by the toolbox. It can also be used to identify the model for prediction.

This package System Identification Toolbox was chosen because of its features:

- the ability to identify the transfer functions of process models and models in the state space according to the response in the frequency and time domain;
- can be used to estimate the autoregression model (ARX, ARMAX), model Box-Jenkins (Box-Jenkins) and Output-Error (Out-error) model using techniques of identification types: maximum likelihood minimization of the predicted error (PEM - prediction-error minimization),the subspace system.;
- simulation of the time sequence (AR, ARMA, ARIMA) and forecasting;
- Identification of Nonlinear ARX models and Hammerstein-Wiener models with nonlinearities in the input and output, such as saturation and 'dead' zone;

- Identification of linear and nonlinear systems like black boxes for evaluate models, user-defined;
- Evaluation of the delays, the trend removal, the filtering,the resampling and the recovery of missing data;
- blocks for the use of the identified models into Simulink.

The aim of this work is the establish the relationship between the electromagnetic processes occurring in friction and electrical characteristics of the memristor.

To address this issue was proposed a method of comparing the estimated value of the electrical contact resistance of the tribopair and resistance of the memristor using the algorithms used in the package System Identification Toolbox.

To obtain the transfer function has been applied the method of "black box" - building a model system using the input and output experimental data (algorithm schematically represented in Figure 32). As input data were used the values of the electrical characteristics of the contact tribopair, in particular the dependence of contact resistance versus time (see in Figure 30 and Figure 31) obtained by an experimental set forth above; as output - the dependence of the resistance change memristora with time obtained in the simulation (Figure 24).

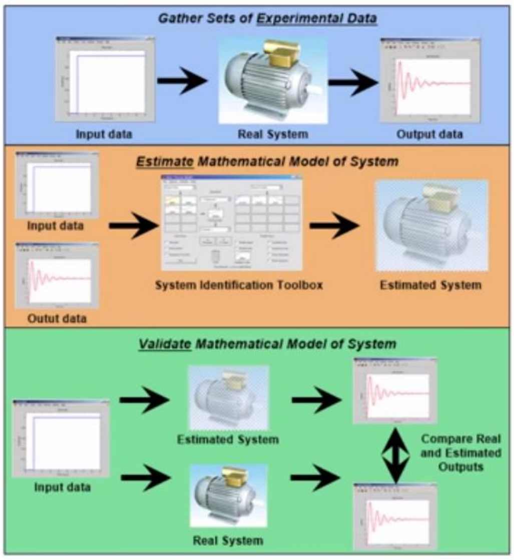

Figure 32 - The algorithm of System Identification Toolbox operation [43]

As a result, there was obtained the transfer function, which describes the relationship between the electrical resistance of contact tribopair and resistance of the memristor.

This transfer function allows to process the incoming characteristics (in this case the dependence of the resistance of the contact tribopair), removes noise and scales the graph to allow further comparison with the function of dependence of the memristance.

Using this transfer function, we built the following graphs of the regularities which are shown in Figure 33 and Figure 34.

Transfer function for friction pair Al_2O_3 - TiN:

$$y(u(r)) = 60 \cdot \left(\frac{-0.101 \cdot r^2 + 0.189 \cdot r + 0.01}{r^3 + 0.0002 \cdot r^2 + 0.00001 \cdot r} + 250 \right) \tag{35}$$

where *y(u(r))* – output function; *u(r)* – input function.

Transfer function for friction pair Al_2O_3 - AlTiN:

$$y(u(r)) = 26 \cdot \left(\frac{0.6694 \cdot r - 0.0333}{r^2 + 0.000006 \cdot r + 0.000144} + 650 \right) \tag{36}$$

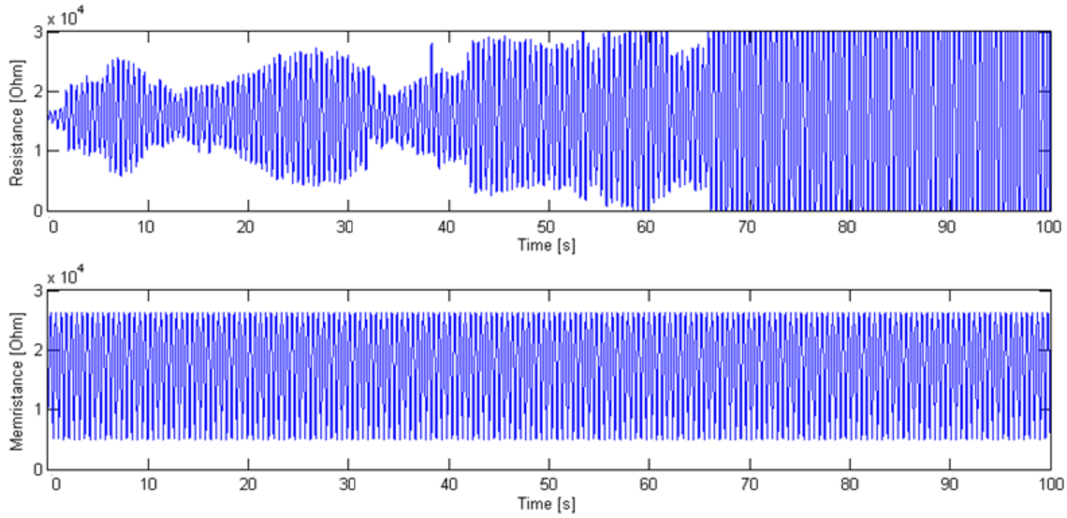

Figure 33 - The result of using transfer function for friction pair Al_2O_3 - TiN: the top graph – modeling of contact resistance change during the friction process; the lower graph - change of memristance.

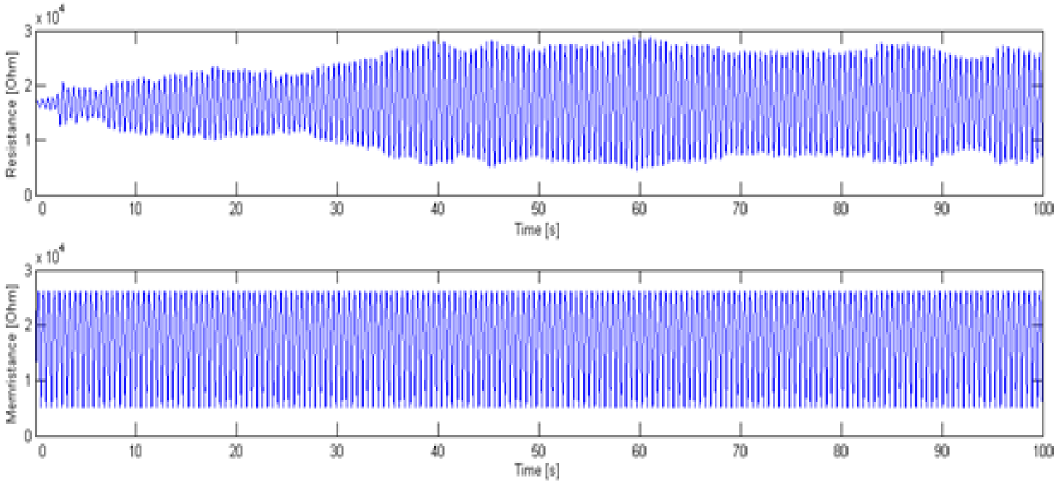

Figure 34 - The result of using transfer function for friction pair Al_2O_3 - AlTiN: the top graph – modeling of contact resistance change during the friction process; the lower graph - change of memristance.

Based on the obtained regularities (see in Figure 33 and Figure 34), we can conclude, that at some point of time, the resistance of the contact area has variation law of electrical characteristics to a high accuracy repeating regularity of change memristance.

5.5. Conclusion of Chapter 5

In this chapter was described the conducted experiments to study the characteristics of the friction pairs. Based on the obtained data was find the transfer function for the assess of the electrical characteristics of the contact of the tribopair and the electrical characteristics of the memristor.

6. The approach of the memristor application in simulation of a friction processes

This chapter describes the using of the proposed method of comparison of the electrical characteristics of the tribopairs of the memristor.

6.1. Comparison of the electrical characteristics of the tribopair contact and the memristor

On the basis of the previous chapter, we can conclude that at certain times moment the electrical contact of triboparis has resistance which repeats with great precision the law of the resistance change of the memristor (memristance). In view of the above said, it has been suggested that at this timepoints the electrical processes which occurring in the contact zone of the tribopair lend itself to the theory of memristance and tribopair can be considered as a kind of the memristor.

In Figure 35 shown the electrical equivalent circuit of the tribopair contact and the same electrical equivalent circuit but with use of the memristor instead the tribopair contact. These models were built to study the changes of the electrical characteristics (voltage drop) in the memristor and the tribopair contact. Actually, the tribopair contact be revealed as a resistor with a value changes over time (variable resistor). Due to similar behavior of the change law of resistance (as described above) the model of the tribopair contact can be replaced by the memristor.

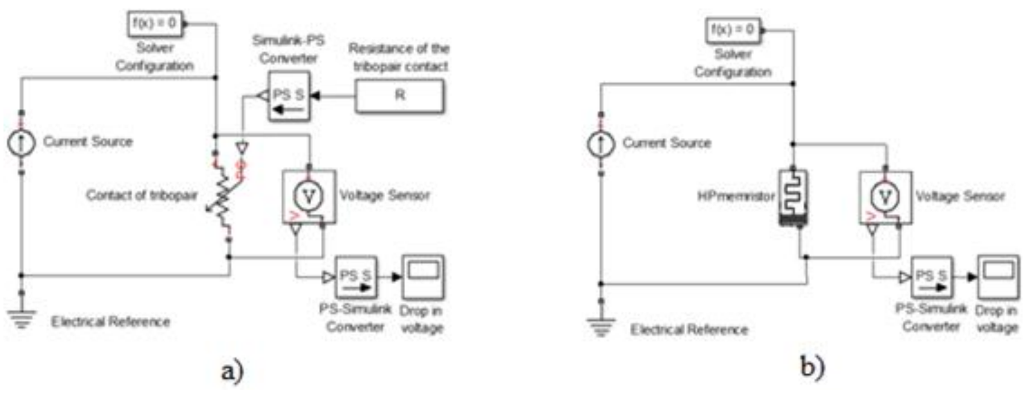

Figure 35 - Electrical equivalent circuit: a) the tribopair contact; b) using the memristor instead of the tribopair contact

In constructing the electrical equivalent circuit model to simulate the resistance of the tribopair was used variable resistor which is had the values obtained by experiment (described in Chapter 5). Block "Current Source" was source of the necessary current. By dint of the block "Voltage Sensor" was measured the voltage drop across tribocontact. Also it was built another model, in which instead of the block "Contact of tribopair" was used the memristor model, which was described above.

Using the dependence of the contact resistance of the triboparah from the Chapter 4, we can assess its electrical characteristics. Under the same conditions of current flow (I = 0.1 A) graphs of the drop in voltage of the tribopairs and of the memristor have the curve shape, shown in Figure 36.

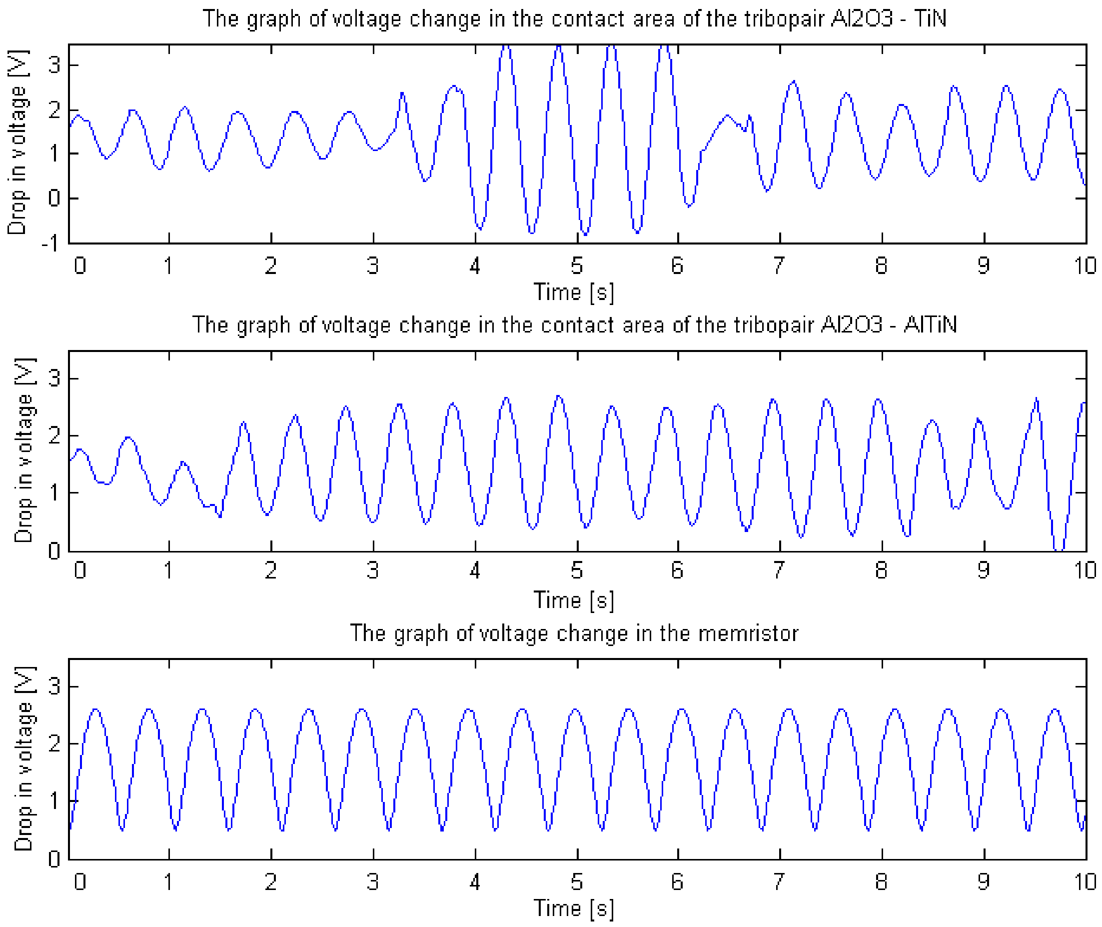

Figure 36 - Drop in voltage of the elements

Analysis of the graphs, shown above, confirms our hypothesis and proves that at certain times the electrical parameters of the tribopair contact is really repeated the properties of the memristor. Also, it can be seen that depending on the used treibopair material the amplitude and the phase diagrams of voltage drop is changing.

It opens up new vistas for the study of electrical phenomena in friction. Using the main properties of the memristor - the memory effect and hysteresis current-voltage characteristics, we can examine in more detail the electrical processes occurring in the friction processes. Also, there is an opportunity to look at a tribological pair in the context of electromagnetic theory.

6.2. Description of the suggested approach

Having regard to the above, it was proposed a method of using the memristor to build an electrical equivalent circuit of the tribopair contact.

The main stages of the approach:

1. A transfer function which is used for communicate of the resistance change of the tribopar contact and the memristance, was searched by dint of using the experimental data which is characterizing the electrical properties of the tribopair contact and the modelled data of the electrical parameters of the memristor.
2. A regularity, between the change of the drop in voltage in the tribopair contact and in the memristor, was searched by dint of using the equivalent circuit of the tribopair contact.
3. Based on the data it is concluded about practicability of using the memristor as a replacement of the tribopair contact in the electric scheme
4. On the basis of a transfer function and the memristor model it can be built a model which with high accuracy will describe the electrical processes occurring in tribocontact during the friction process. Due to the memristance effect, it's possible to take into account of the influence of the processes was occurred previously. However, this stage is still poorly understood and requires further study.

6.3. Conclusion of Chapter 6

In this chapter was described the method of comparing the electrical characteristics of the tribopair contact and electrical characteristics of the memristor. There was given the electrical equivalent circuits for the tribopair contact. On the basis of these schemes was compared the drop in voltage on the memristor and on the tribopair contact.

Conclusions

According to this work, the electrical phenomena, such as frictional electricity, thermal electromotive force, and others originate in the friction process. It is shown that these processes affect the tribological characteristics of friction bodies. Currently, the electromagnetic phenomena occurring in the process of the friction very complicated and insufficiently studied, therefore subject of this work is quite relevant.

In the course of the works, it has been proposed the approach, whereunder during the simulation of the process of friction, the memristor can replace the contact of the friction pair, also its using will be help in the investigation of the tribocontact in the context of electrical circuits. There was deduced that the electrical characteristics of the tribopair contact is repeating with high precision the electrical characteristics of the memristor. In the work was noted that the electromagnetic phenomena influence on the characteristics of the friction pair. However, comparing the electrical characteristics of the data (of the tribocontact and the memristor) may be determined the parameters of electrical phenomena in friction. It provides the new opportunities for the study of electrical phenomena during friction.

Future work

This study is the first stage in the study of electrical phenomena through modeling of friction using the memristor. The proposed method requires further detailed examination to definitively draw conclusions about the relevance of use.

As further work there is necessary to investigate the influence of all parameters was measured during friction (friction force, wear, elastic modulus, hardness, etc.) on the electrical characteristics of the contact friction pair.

After that we will be able to evaluate in full the characteristics of the electrical processes in friction and compare the obtained data with the theory of the memristor.

References

1. Menguy C. *Encyclopedia of Occupational Health and Safety*. International Labor Organization, Geneva, 2011. Internet access - *http://www.ilo.org/iloenc/part-vi/electricity/item/400-static-electricity.*
2. An Encyclopedia Britannica Company. Internet access - *http://www.merriam-webster.com/dictionary/friction.*
3. Chebotarev Y. *Classification of electromagnetic phenomena in triboengineering*. Vestnik DSTU, vol. 6, № 1 (28), 2006, pp. 78-81.
4. Khebda M.; Chichinadze A. *Tribotechnology reference guide.* Manufacturing engineering, Moscow, 1989, pp. 75 - 78.
5. Mashkov K. *Tribophysics of metals and polymetric compounds*. Monograph, Publishing house OmSTU, Omsk, 2013.
6. Mashkov J.; Blesman A. *Dynamics of the friction process of metal-polymer tribosystems*. Manufacturing engineering, Moscow, vol. 4, 1990, pp. 244-253.
7. Postnikov S. *Electrical Phenomena in Friction and Cutting*. Publishing house Volgo-Vyatsk, Gorky, 1975.
8. Leb L. *Static electrification.* Moscow, GEU, 1963.
9. Bowden F.; Tabor D. *Friction and lubrication.* Moscow, Mashgiz, 1960.
10. Harper W. *The generation of static charge*. Publisher TAYLOR&FRANCIS LTD, vol.6, Issue 24, 1957, pp. 365-417.
11. Kornfeld M. *Solid-state physics.* I., vol. 11, Issue 6, 1969, pp. 1611-1616.
12. Gordienko P.; Gordienko S. *The influence of the electric current on the wear by friction of the metal bodies.* Herald Engineering, vol. 7, 1952, p. 38.
13. Korshunov L.; Minz R. *The impact of electrification and small direct currents on the wear of metals in sliding friction.* Physicochemical mechanics of materials, vol. 3, Issue 4, 1967, pp. 392-396.
14. Galey M. *The wear resistance of tools and electrical phenomena in the chain of the machine - the product - a tool.* Technology of instrument, vol. 8, 1965, pp. 16-19.
15. Polyakov A. *Investigation of a hydrogen wear*. Moscow: Science, 1977.
16. Evdokimov V. *Exoelectron emission during a friction*. Moscow: Science, 1973.

17. Rizhkin A. *The effect of plastic deformation on the thermal regime of the friction zone*. Rostov-on-Don, RISXM, 1980, pp. 87- 89.
18. Dubinin A. *The friction and wear in machine components*. Moscow: Mashgiz, 1952.
19. Dubinin A. *Energy of the friction and wear of machine parts*. Moscow: Mashgiz, 1963.
20. Gordienko P. *The effect of the electric current on the mechanical wear during friction of bodies*. Engineering herald, vol. 7, 1952, pp. 23-25.
21. L. Chua. *Memristor - the missing circiut element*. IEEE Trans. Circuit Theory, vol. CT-18, 1971, pp. 507-519.
22. Mullians J. *Memristive minds*. Internet access - http://nature.berkeley.edu/Memristor.pdf.
23. Strukov D.; Gregory S.; Duncan S. eds. *The missing memristor found*. Nature, vol. 453, 2008, pp. 80-83.
24. Mazumder P.; Kang S.; Waser R. *Memristors: Devices, Models, and Applications*. Proceedings of the IEEE , vol. 100, Issue 6, June 2012, pp. 1911-1919.
25. Kvatinsky S.; Friedman E.; Kolodny A. and Weiser U. *Memristors and Related Applications.* The International Conference of the Israeli Semiconductor Industry (ChipEx 2011), May 2011.
26. Kumar A. *Memristor: The 4th Circuit Element*. International Journal of Advanced Computer and Mathematical Sciences, vol. 3, Issue 1, 2012, pp. 176-180.
27. Nuzhdin K.; Stepanov M. *Applicability of Memristors for Research of Friction Processes.* Closing Conference of the Project, Doctoral school of energy and geotechnology II, Parnu, Estonia, January 12-17, 2015, pp. 195-200.
28. Chua L.; Kang S. *Memristive devices and systems*. Proc. IEEE, vol. 64, 1976, pp. 209 – 223.
29. Rajendran, J.; Harika M.; Ramesh K. and Garrett S. An energy-efficient memristive threshold logic circuit, IEEE Transactions on Computers, vol. 61, 2012, pp. 474-487.

30. Robinson E. *Compact method for modeling and simulation of memristor devices: Ion conductor chalcogenide-based memristor devices*. IEEE/ACM International Symposium on Nanoscale Architectures, 2010, pp. 1 - 4.
31. Eliseev, N. *Memristors and crossbars: nanotechnology for processors*. ELECTRONICS: Science, Technology, Business, 2010, pp. 84 - 89.
32. Williams S. *How We Found the Missing Memristor*. IEEE Spectrum, December 2008.
33. Surabathula K. *Memristor the fourth fundamental electronic element*. 2010, pp. 8 – 13.
34. Hutchby J. *Electrochemical metalization, Atomic Switch diagram. Phase change and nanoionic memory cells.* 2010. Internet access - http://electronics.wesrch.com/pdfEL1SE1000YKZZ.
35. *Memristor. Production of the structure and studying its properties.* Laboratory workshop for the 5th year FFKE MIPT, Dolgoprudny, 2013.
36. Matrix Laboratory. Internet access - *https://ru.wikipedia.org/wiki/MATLAB#.D0.98.D0.BD.D1.82.D0.B5.D1.80.D0.B5.D1.81.D0.BD.D1.8B.D0.B5_.D1.84.D0.B0.D0.BA.D1.82.D1.8B*
37. Chernyh I. *Simulink: simulation tool of dynamic systems*. Internet access - *http://matlab.exponenta.ru/simulink/book1/.*
38. Model of the memristor by Thang Hoang. Internet access - *http://cn.mathworks.com/matlabcentral/fileexchange/25082-memristor-model.*
39. Zhang H.; Gao B.; Sun B. et al. *Ionic doping effect in* ZrO_2 *resistive switching memory*. Appl. Phys. Lett. 96, 123502, 22 March 2010.
40. Zanaveskin M.; Khrapovitskaya Y.; Maslova N.; Emelianov A. et al. *Influence of structural parameters of the memristor based on titan on its electrical characteristics*. Software systems: theory and applications, vol. 3(17), 2013.
41. Manual tribometer type TRM 1000, WAZAU company, Rev. 02.2007.
42. Berkovich I.; Gromakovsky D. Tribology. Physical basis, mechanics and technical applications. Textbook for high schools, SSTU, Samara, 2000.
43. Webinar. *System Identification Toolbox*. Internet access - *https://www.youtube.com/watch?v=bCBRZNoGyA8.*